Geological Paper GP85-1

Sapphirine Coronas from Sipiwesk Lake, Manitoba

By J.J. Macek

Manitoba
Energy and Mines
Geological Services

1989

This publication is available in large print, audiotape or braille on request.

Manitoba
Energy and Mines
Geological Services

Geological Paper GP85-1

Sapphirine Coronas from Sipiwesk Lake, Manitoba

By J.J. Macek

Winnipeg, 1989

Energy and Mines

Hon. Harold J. Neufeld
Minister

Ian Haugh
Deputy Minister

Minerals Division

Sobharam Singh
Assistant Deputy Minister

Geological Services
W.D. McRitchie
Director

90-06383/1

TABLE OF CONTENTS

	Page
ABSTRACT	1
INTRODUCTION	2
Previous Work	2
Acknowledgements	2
GEOLOGICAL DESCRIPTION	3
TEXTURAL OBSERVATIONS AND IMPLICATIONS	4
Phlogopite-spinel-orthopyroxene granulite	4
Phlogopite-sapphirine-orthopyroxene granulite	4
Relationship between ultramafic granulite and mobilizate	4
Coronas	5
Cordierite corona	5
Sillimanite-cordierite corona	5
Sillimanite-orthopyroxene corona	5
Sillimanite-garnet corona	6
Garnet corona	6
Summary of suggested equations	7
Feldspar crystallization	7
Symplectites	7
Interpretation of the petrological processes from the textural and mineralogical evidence	7
Minerals in possible equilibrium	9
CONCLUSIONS	10
REFERENCES	11
APPENDIX A: Whole rock chemical analyses	29
APPENDIX B: Mineral microprobe analyses	31

LIST OF FIGURES

Figure 1:	A boudinaged end of disrupted layered ultramafic-mafic granulite intruded by leucocratic mobilizate	12
Figure 2:	Layered felsic to mafic granulite sequence locally severely tectonized and intruded by leucocratic mobilizate	12
Figure 3:	Leucocratic mobilizate carrying numerous ultramafic to felsic fragments, termed "mobilizate melange"	12
Figure 4:	Schematized geological relationships of common principal lithological units	13
Figure 5:	Phlogopite-spinel-orthopyroxene granulite	14
Figure 6:	Lepidogranoblastic texture of phlogopite-spinel-orthopyroxene granulite	15
Figure 7:	Rutile needles enclosed in orthopyroxene	15
Figure 8:	Incipient formation of sapphirine between phlogopite and spinel	15
Figure 9:	Sapphirine formation from spinel and phlogopite. Phlogopite is distinctly corroded	16
Figure 10:	Incipient formation of sapphirine from spinel and phlogopite	16
Figure 11:	Formation of sapphirine from spinel and phlogopite	16
Figure 12:	Granoblastic texture of phlogopite-sapphirine-orthopyroxene granulite	17
Figure 13:	Areas of plagioclase and cordierite represent embayments originally filled with mobilizate	17
Figure 14:	Mobilizate-ultramafic granulite contact	17
Figure 15:	Subhedral crystal of sapphirine "broken off" at the contact between ultramafic granulite and mobilizate	18
Figure 16:	Quartz in mobilizate 15-25 cm away from ultramafic granulite	18
Figure 17	a):Contact between ultramafic (phlogopite-spinel-orthopyroxene) granulite and mafic granulite before intrusion of mobilizate	19
	b):Mobilizate, which contained free silica, intruded along the contact of the ultramafic-mafic pair	19

Page

Figure 18: Incomplete rim of cordierite around sapphirine crystal 20
Figure.19: Graphical relationship of spinel, sapphirine, cordierite and sillimanite in the SiO_2-(Mg, Fe)O-Al_2O_3 system 20
Figure 20: Plot of the sapphirine compositions 21
Figure 21: Sillimanite-cordierite corona 22
Figure 22: Sillimanite-orthopyroxene corona. Sillimanite rim consists of few mono-crystals 22
Figure 23: Sillimanite-orthopyroxene corona 22
Figure 24 a):Garnet-orthopyroxene corona 23
b):Same object in Figure 24 under crossed nicols 23
Figure 25: Sillimanite-garnet corona 24
Figure 26: Garnet formation from sapphirine 24
Figure 27: Spinel overgrown by garnet or enclosed by plagioclase 25
Figure 28: Sapphirine enclosed in plagioclase and/or garnet 25
Figure 29: Sapphirine rimmed by cordierite corona serves as crystallization centre for subsequent crystallization of plagioclase and potassium feldspar 25
Figure 30: Relicts of two sapphirine crystals rimmed by cordierite coronas that are in turn mantled by plagioclase 26
Figure 31: Symmetrical mineral zoning around sapphirine crystal relicts 26
Figure 32: Orthopyroxene-sillimanite symplectite enclosed in cordierite 26
Figure 33: Ornamental relict of sillimanite enclosed in cordierite and resembling symplectite 27
Figure 34: Contact of sapphirine orthopyroxenite with mobilizate 27
Figure 35: Elongate and deformed spinel orthopyroxenite fragments in "mobilizate melange" 27
Figure 36: Corundum grain surrounded by cordierite 36
Figure 37: Plot of all chemical analyses in the SiO_2-(Mg,Fe)O-Al_2O_3 diagram. (in Appendix A) 28

LIST OF TABLES

Table 1: Granulites - mineral assemblages 3
Table 2: Minerals in equilibrium under given P-T- conditions 9

ABSTRACT

Spinel-bearing ultramafic granulites at Sipiwesk Lake (Manitoba) were intruded by melts containing free silica, resulting in spinel being transformed partially or completely into sapphirine. The sapphirine reacted, in turn, with the continuously evolving melt of varied silica activity producing several reaction coronas. Three major factors guided the formation of the coronas, as deduced from microscope observations: 1) decreasing silica activity of the melt, 2) varied viscosity of the melt, and 3) a minor variation in the aluminum content of the sapphirine. Textural evidence suggests that only one mineralogical phase reacted at a time with the silica component while the other minerals remained passive. Thus, it appears that metamorphic grids, constructed on the assumption that every observed mineral phase is the result of synchronous reactions, cannot be directly applied to the Sipiwesk locality.

INTRODUCTION

The occurrence of sapphirine in rocks substantially enriched in magnesium and aluminum is commonly interpreted as an indicator of extremely high P-T metamorphic conditions. Numerous studies have attempted to apply knowledge gained from experimental systems to the natural sapphirine-bearing paragenesis in order to determine metamorphic conditions of a particular terrain. The derived conclusions are frequently tentative as they are based on a number of arbitrary assumptions. These assumptions are usually clearly stated and thus the limitations of a given interpretation can be readily evaluated. However, studies rarely provide sufficient petrographic descriptions nor a complete photomicrographic record in support of the proposed mineralogical reactions.

The purpose of this paper is to provide a basic petrographic record of the Sipiwesk sapphirine occurrence and also to point out some deficiencies of the traditional approach.

Previous Work

Sapphirine on Sipiwesk Lake was first identified by Hubregtse (1978) and subsequently placed in a geological and metamorphic context (Hubregtse, 1980). A number of samples were analyzed for major elements by microprobe analysis. Sample selection attempted to characterize the chemical range of granulites and also to provide crystallochemical data about minerals of the sapphirine-bearing paragenesis. The present study was undertaken to extend the documentation and interpretation of the sapphirine-bearing gneisses.

The only paper concerned with establishing the P-T conditions of the sapphirine-bearing granulites on Sipiwesk Lake was published by Arima and Barnett (1984). Their results are discussed in some detail later.

Acknowledgements

The sapphirine project was initiated by J.J.M.W. Hubregtse as an ancillary to his regional mapping in the Pikwitonei granulite domain in the Superior Province. His contribution facilitated a sound structural and metamorphic historical framework that will benefit all future investigations.

Ron Chapman from the University of Manitoba did all microprobe analyses. Whole rocks chemical analyses were done by the Manitoba Energy and Mines Analytical Laboratory, Logan Avenue, Winnipeg.

The author also wishes to thank his colleagues M.T. Corkery, W. Weber, B.B. Bannatyne, W.D. McRitchie and D.A. Baldwin for critically reading the manuscript, numerous suggestions and helpful discussions. Their input has considerably improved the final product. L. Chudy and S. Weselak typed the various drafts of the manuscript.

GEOLOGICAL DESCRIPTION

Sapphirine-bearing rocks are exposed on several outcrops south of The Narrows in central Sipiwesk Lake, (latitude 55°06'30", longitude 97°30'40").

Sapphirine is closely associated with layers of ultramafic rock, which are part of an ultramafic-mafic sequence hosted by leucocratic, strongly foliated and homogeneous granulite gneiss of variable composition.

Although the mafic and ultramafic layers form a well defined unit hundreds of metres in length, significant disruptions occur along strike. Layers are commonly segmented, boudinaged (Fig. 1, 2) and tightly folded. Tectonic pressure shadows around ultramafic boudins are filled with coarse grained leucocratic mobilizate that contains numerous mafic and ultramafic inclusions that are compositionally identical to the segmented layers (Fig. 3). This "mobilizate melange" originated during deformation when fragments were formed from more competent ultramafic and mafic layers and these were engulfed by intruding mobilizate.

Four distinct lithological units can be defined:

A. ultramafic granulites
B. mafic granulites
C. leucocratic granulites
D. mobilizate and/or "mobilizate melange"

The typical relationships displayed by these units are schematically depicted in Figure 4. Sapphirine occurs exclusively in marginal zones of spinel-bearing ultramafic granulite and in mobilizate and/or "mobilizate melange" closely associated with such ultramafic granulite. Other granulites and mobilizate are sapphirine-free.

Although only four principal rock units are shown in Figure 4, a variety of mineral assemblages are found within each of the four units. The most common assemblages are listed in Table 1, while Figure 37 shows their range in chemistry.

TABLE 1
Granulites - mineral assemblages
(modal percentages are indicated in brackets)

A. Ultramafic granulites
   1. Phl-Spl-Opx granulite (15-25-60)
   2. Phl-Spr-Opx granulite (3-25-72)

B. Mafic granulites
   1. Mag-Qtz-Opx granulite (7-8-40-45)
   2. Mag-Qtz-Pl-Cpx-Opx granulite (7-8-35-5-45)
   3. Mag-Cpx-Opx-Pl granulite (5-10-20-65)

C. Leucocratic granulites
   1. Mag-Grt-Opx-Qtz-Pl granulite (5-7-8-20-60)
   2. Crd-Sil-Opx-Kfs-Qtz granulite (5-10-15-10-60)
   3. Bt-Crd-Kfs-Sil-Opx-Qtz granulite (5-7-3-15-50-20)
   4. Grt-Kfs-Qtz granulite (3-2-95)
   5. Opx-Kfs-Qtz granulite (10-30-60)
   6. Grt-Qtz-Pl granulite (10-35-55)
   7. Opx-Qtz-Kfs granulite (5-30-65)
   8. Bt-Opx-Qtz-Pl granulite (10-25-25-40)
   9. Bt-Opx-Crd-Kfs-Qtz granulite (5-5-20-5-65)

D. Mobilizate and/or "mobilizate melange" (square brackets designate porphyrocrysts)

   Mobilizate
   1. Qtz-Pl-Kfs + [Opx] ± [Bt]
   2. Qtz-Pl ± [Bt]
   3. Pl-Kfs + [Opx]

   "mobilizate melange"
   1, 2 or 3 + ultramafic fragments
   + mafic fragments
   + single crystals: Opx, Grt, Spr, Spl, Crd, Crn, Phl, Sil
   + coronas: Spr/Crd; Spr/Sil/Crd; Spr/Sil/Opx; Spr/Sil/Grt; Spr/Grt; Spr/Sil
   + symplectites: Opx + Sil, Sil + Crd

NOTE: Abbreviations (also used elsewhere in the text): Ab (albite), An (anorthite), Bt (biotite), Crd (cordierite), Crn (corundum), Grt (garnet), Ksp (K-feldspar), Mag (magnetite), Opx (orthopyroxene), Phl (phlogopite), Pl (plagioclase), Qtz (quartz), Rt (Rutile), Spr (sapphirine), Sil (sillimanite), Spl (spinel).

TEXTURAL OBSERVATIONS AND IMPLICATIONS

Phlogopite-spinel-orthopyroxene granulite

The Phl-Spl-Opx granulite forms a single conspicuous layer up to 15 cm thick, that weathers a very dark brown. The unit is medium grained, with a planar foliation emphasized by streaky aggregates of black spinel 4 to 40 mm long (Fig. 5). The pertinent microscopic features are described below. The texture (Fig. 6) is lepidogranoblastic.

Spinel forms dark green polygonal grains clustered into elongated aggregates. Grains are clouded with opaque dust that preferentially occurs along (111) cleavage. Spinel locally encloses corundum and phlogopite laths. Incipient hematitization is observed in some larger opaque (magnetite) grains.

Corundum commonly occurs as clear, rounded, drop-like or polygonal grains enclosed by spinel and orthopyroxene. It may also occur in contact with phlogopite.

Phlogopite forms subhedral laths, enclosed by spinel and orthopyroxene, or cutting across mineral boundaries.

Orthopyroxene occurs as polygonal grains with intense pink (α)-colourless (β,γ) pleochroism. It contains numerous rutile needles (Fig. 7) oriented in [001], [010] and [011].

Phlogopite-sapphirine-orthopyroxene granulite

Phl-Spr-Opx granulite forms a 2-3 cm thick transition zone around the Phl-Spl-Opx granulite layer. It is in this envelope where the conditions for sapphirine formation occurred.

A gradual transition from Phl-Spl-Opx granulite to the Phl-Spr-Opx granulite is characterized by the following changes in mineralogy and textures:

1. Incipient formation of sapphirine is invariably observed at the contact between spinel and phlogopite (Figs. 8, 9,10, 11). Phlogopite displays concave "corrosive" shapes (Fig. 9).
2. Sapphirine progressively replaces spinel and corrodes phlogopite. Where spinel is replaced, phlogopite modal content is reduced from 15 to 1-3% (Fig. 12). The remaining phlogopite forms oval relicts that are 1/4 to 1/10 of the original size.
3. The modal content and the crystal form of corundum appears to be unaffected in the transition zone (Fig. 12).
4. Rutile forms discrete polygonal grains (Fig. 12); many orthopyroxene grains have outer zones free of rutile needles.

These textural and mineralogical observations suggest that sapphirine is formed from spinel by pirating SiO_2 from phlogopite, according to the reaction:

$$Spl + \underset{(Phl)}{SiO_2} \longrightarrow Spr$$

Robertson (1977) lists the stoichiometric equation for the formation of phlogopite that suggests SiO_2 is released if the reaction is reversed.

$$\underset{\text{enstatite}}{5MgSiO_3} + \underset{\text{spinel}}{MgAl_2O_4} + K_2O + 2H_2O + SiO_2 = \underset{\text{phlogopite}}{K_2Mg_6Si_6Al_2O_{20}(OH)_4}$$

This would require the formation of orthopyroxene.

There is no direct microscopic evidence that a new orthopyroxene is obtained from chemical decomposition of phlogopite; it is possible that orthopyroxene could be added to existing grains as an outer rim. Liberated K_2O and H_2O and other volatiles contained in phlogopite would migrate out of the rocks without leaving a trace. Since neither free SiO_2 nor cordierite is available for forming sapphirine from spinel in the Phl-Spl-Opx granulite, it must be concluded from the microscopic evidence that SiO_2 was obtained from phlogopite breakdown.

Relationship between ultramafic granulite and mobilizate

The contact between Phl-Spr-Opx granulite and mobilizate is macroscopically simple (see Fig. 34), but it is microscopically defined as a complex bay-like suture separating Phl-Spr-Opx granulite from areas of mobilizate now filled with plagioclase, potash-feldspar and secondary cordierite (Fig. 13, 14). The following mineralogical and textural features are observed at this contact:

1. Phlogopite forms laths that are comparable in size, shape and modal amount to those in Phl-Spl-Opx granulite. Compare Figure 13 (left part) with Figure 6.
2. Sapphirine forms subhedral to euhedral crystals up to 4 mm long; they are comparable in size to spinel aggregates in Phl-Spl-Opx granulite. These crystals growing out from Phl-Spr-Opx granulite tend to develop euhedral shapes into the mobilizate and are often broken-off and included in mobilizate (Fig. 14). Many of these broken-off crystals are aligned subparallel to the contact (Fig. 15).
3. Quartz first occurs in mobilizate 15-25 cm from the contact (Fig. 16) where sapphirine is absent. Quartz is not observed at the contact.
4. Sapphirine is armored by simple or complex coronas (Table 1). Several types of coronas are observed in a hand specimen and a thin section of "mobilizate melange".

The mode of sapphirine development at the contact of ultramafic granulite layers with mobilizate is suggested by the following observations:

1. Preservation of phlogopite near the contact indicates that it was not involved in sapphirine development;
2. Absence of quartz directly at the contact, and occurrence of quartz at some distance from the contact in the mobilizate; and
3. Tendency of sapphirine to develop as idiomorphic crystals.

These observations support the following reaction:

$$Spl + \underset{(mob.)}{SiO_2} \longrightarrow Spr$$

The suggested different origin of sapphirine within the Phl-Spl-Opx granulite, as opposed to that at its contacts with mobilizate, is schematically shown in Figure 17.

Coronas

As previously indicated, coronas on sapphirine develop only in "mobilizate melange" (Table 1). They originated through interactions of mobilizate with newly formed crystals of sapphirine. Coronas originating from other minerals (Opx, Grt, Crn, Sil) were not detected.

The types of observed coronas are presented on photomicrographs (Fig. 18 and 21 to 26), and their modes of formation are suggested through manipulation of simplified chemical formulae.

Cordierite corona

Sapphirine rimmed by cordierite (Fig. 18) is mineralogically the simplest corona. Such coronas usually occur close to the contact between ultramafic granulite and mobilizate. Ideally, the origin of cordierite coronas can be explained by the following scheme:

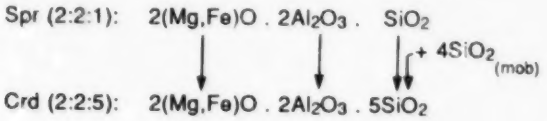

This scheme results in the following equation:

$$\text{Spr (2:2:1)} + 4SiO_{2\,(mob.)} \longrightarrow \text{Crd (2:2:5)}$$

Sillimanite-Cordierite corona

The cordierite corona equation is valid for an ideal sapphirine (2:2:1) situated directly on the tieline connecting spinel (1:1:0), cordierite (2:2:5) and quartz in the SiO_2-(Mg,Fe)O-Al_2O_3 system (Fig. 19). If a more aluminous sapphirine is considered an excess of aluminum oxide must result.

Figure 20 shows the twelve sapphirine microprobe analyses plotted on the SiO_2-(Mg,Fe)O-Al_2O_3 diagram. A departure of the plotted points from an ideal (2:2:1)-(3:5:1) compositional line is caused by expressing total iron as FeO. If the presence of Fe_2O_3 is considered the plotted points would likely shift subhorizontally close to, or on the (2:2:1)-(3:5:1) compositional line (cf. Mohan et al., 1986). From Figure 20 it is apparent that analyzed sapphirine compositions range from (6-1/3:7:3) to (7:9:3) ratios.

Employing (7:9:3) ratio and simplifying it to (2:3:1) to avoid fractions, a scheme analogous to the cordierite corona may be devised:

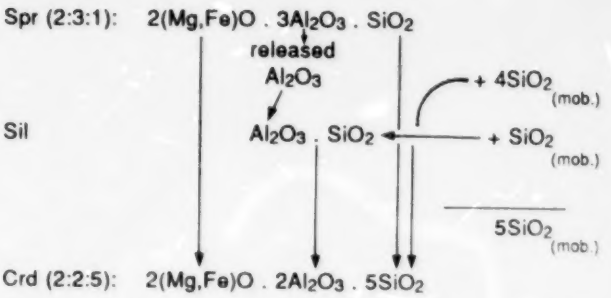

According to this scheme sillimanite is formed in addition to cordierite and is situated between sapphirine and newly crystallized cordierite according to the equation:

$$\text{Spr (2:3:1)} + 5SiO_{2\,(mob.)} \longrightarrow \text{Sil} + \text{Crd (2:2:5)}$$

Figure 21 shows an example of this type of corona.

Sillimanite-orthopyroxene corona

Another type of corona, commonly observed in mobilizate, is the sillimanite-orthopyroxene combination (Fig. 22, 23). Here sillimanite is formed between sapphirine and orthopyroxene. Depending on the composition of the sapphirine a series of possible reactions may be considered. Two previously introduced sapphirine compositions are used again in the schemes below:

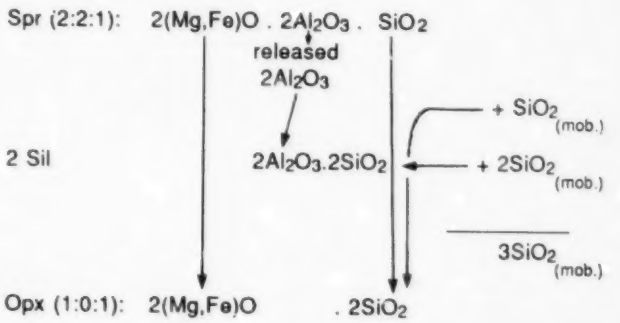

and

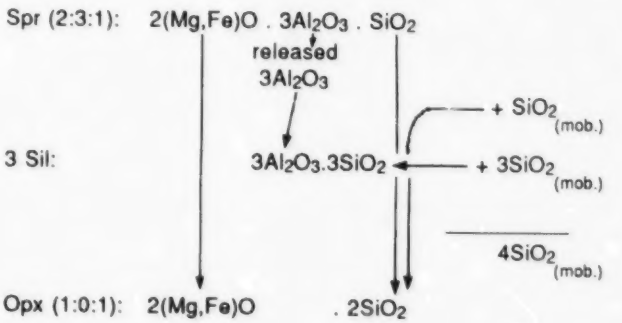

leading to two equations respectively:

$$\text{Spr (2:2:1)} + 3SiO_2 \xrightarrow[\text{(mob.)}]{} 2\ \text{Sil} + \text{Opx}$$

and

$$\text{Spr (2:3:1)} + 4SiO_2 \xrightarrow[\text{(mob.)}]{} 3\ \text{Sil} + \text{Opx}$$

The mobilizate provides the required silica to balance the equations and thus explain the physical relationships observed in the corona development.

Sillimanite-garnet corona

Sillimanite and garnet (Figs. 24-25) form another commonly observed corona on sapphirine. Once more, simple ideal formulae are used:

Spr (2:2:1): $2(Mg,Fe)O \cdot 2Al_2O_3 \cdot SiO_2$

and

Grt (3:1:3): $3(Mg,Fe)O \cdot Al_2O_3 \cdot 3SiO_2$

In order to work with equal amounts of Mg and Fe cations, formulae are multiplied by 3 and 2 respectively:

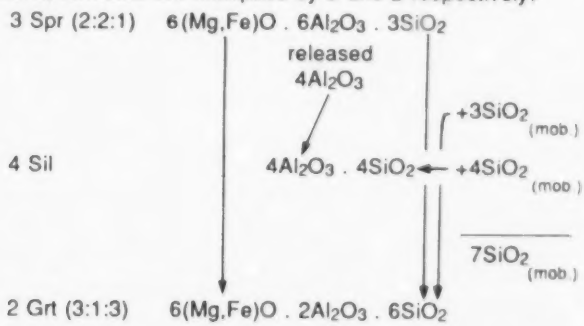

and

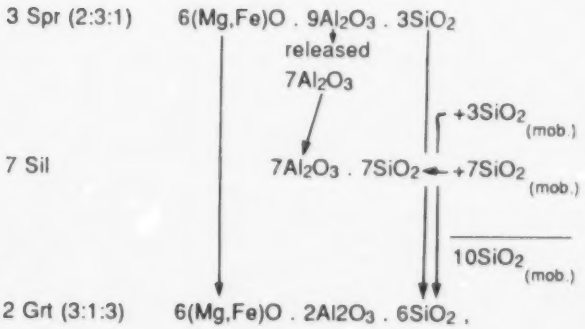

leading to two equations respectively:

$$3\ \text{Spr (2:2:1)} + 7SiO_2 \xrightarrow[\text{(mob.)}]{} 4\ \text{Sil} + 2\ \text{Grt (3:1:3)}$$

and

$$3\ \text{Spr (2:3:1)} + 10SiO_2 \xrightarrow[\text{(mob.)}]{} 7\ \text{Sil} + 2\ \text{Grt (3:1:3)}$$

To compare the above equations on the basis of one sapphirine formula as in the preceding discussion, the equations are transposed into the following final forms:

$$\text{Spr (2:2:1)} + 2\ 1/3\ SiO_2 \xrightarrow[\text{(mob.)}]{} 1\ 1/3\ \text{Sil} + 2/3\ \text{Grt (3:1:3)}$$

and

$$\text{Spr (2:3:1)} + 3\ 1/3\ SiO_2 \xrightarrow[\text{(mob.)}]{} 2\ 1/3\ \text{Sil} + 2/3\ \text{Grt (3:1:3)}$$

Garnet corona

In one thin section (Fig. 26) sillimanite is restricted to a narrow rim observed on some sapphirine crystals. In another part of the this section sapphirine appears to have been transformed directly into garnet. Considering the chemical scheme involving sapphirine (2:2:1) that is transformed into sillimanite + garnet, and observing that sillimanite is not found, nor any other aluminous phase such as corundum in the vicinity of the garnet corona, it is reasonable to interpret that there was not enough silica in the mobilizate to provide for sillimanite formation. The lack of corundum would suggest that the P-T conditions were not suitable for corundum formation and that the excess of Al_2O_3 was absorbed by the feldspar component in the $(K,Na)_2O$-CaO-Al_2O_3-SiO_2 system.

This could be expressed by the following theoretical scheme:

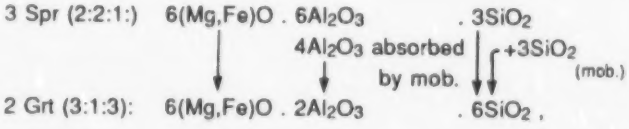

leading to the following equation:

$$3\ \text{Spr (2:2:1)} + 3SiO_2 \xrightarrow[\text{(mob.)}]{} 2\ \text{Grt (3:1:3)} + 4Al_2O_3\ \text{(absorbed by mob.)}$$

and equivalently:

$$\text{Spr (2:2:1)} + SiO_2 \xrightarrow[\text{(mob.)}]{} 2/3\ \text{Grt (3:1:3)} + 1\ 1/3\ Al_2O_3\ \text{(absorbed in mob.)}$$

Summary of suggested equations

Textural evidence, together with the derived equations, permits the following summary of reactions:

	Σ of Free SiO_2 required
Ultramafic granulite:	
central zone: no reaction	0
border zone: $Spl + SiO_2 \xrightarrow[(Phl)]{} Spr$	0
Contact:	
buffered reaction: $Spl + SiO_2 \xrightarrow[(mob.)]{} Spr$	1
Mobilizate:	
$Spr\ (2:3:1) + 5SiO_2 \xrightarrow[(mob.)]{} Sil + Crd\ (2:2:5)$	6
$Spr\ (2:2:1) + 4SiO_2 \xrightarrow[(mob.)]{} Crd\ (2:2:5)$	5
$Spr\ (2:3:1) + 4SiO_2 \xrightarrow[(mob.)]{} 3Sil + Opx\ (1:0:1)$	5
$Spr\ (2:3:1) + 3\ 1/3\ SiO_2 \xrightarrow[(mob.)]{} 2\ 1/3\ Sil + 2/3\ Grt\ (3:1:3)$	4⅓
$Spr\ (2:2:1) + 3SiO_2 \xrightarrow[(mob.)]{} 2Sil + Opx\ (1:0:1)$	4
$Spr\ (2:2:1) + 2\ 1/3\ SiO_2 \rightarrow 1\ 1/3\ Sil + 2/3\ Grt\ (3:1:3)$	3⅓
$Spr\ (2:2:1) + 1\ SiO_2 \xrightarrow[(mob.)]{} 2/3\ Grt\ (3:1:3) + 1\ 1/3\ Al_2O_3$ (abs. in mob.)	2

It is apparent that the major factor in formation of various coronas surrounding sapphirine in mobilizate is a gradually decreasing silica activity in the mobilizate coupled with a variation in sapphirine composition. Sapphirine as such is thus strictly a transient mineral phase that is preserved only by the coincidence of an insufficient supply of silica and rapidly dissipating heat energy.

The textural evidence of complete silica exhaustion in the mobilizate is shown in Figure 27. Spinel grains are overgrown by garnet or surrounded by plagioclase. If silica was available in the mobilizate, spinel should be rimmed by sapphirine. Spinel served as a crystallization centre for garnet that crystallized from locally concentrated ions of appropriate composition. Another example of the silica depletion is shown in Figure 28. In this case sapphirine is surrounded by plagioclase, and nearby, another sapphirine is overgrown by garnet. In the latter case it cannot be clearly demonstrated that some silica was available locally for at least partial formation of garnet according to the last equation.

Feldspar crystallization

Exhaustion of free silica in mobilizate had ended crystallization in the SiO_2-(Mg,Fe)0-Al_2O_3 system.

Figures 29 to 31 show the results of the crystallization of the residual liquid. The composition of this liquid belonged to the $(Na,K)_2O$-CaO-Al_2O_3-SiO_2 system and produced feldspars. Plagioclase An_{35-40} mantles cordierite coronas on sapphirine and encloses pods of perthite. Plagioclase crystallized first using the existing minerals and coronas as crystallization centres. Considering the composition of the plagioclase this residual liquid was fairly basic. Plagioclase and potassium feldspar are not parts of coronas; therefore their crystallization is not further discussed.

Symplectites

Symplectites were found in thin sections from one of Hubregtse's grab samples, the location of which is not exactly known. The mineralogy suggests that the symplectites belong to highly siliceous mobilizate. It is impossible to determine whether mobilizate contained some spinel or p[illegible]-crysts of sapphirine derived from an ultramafic layer. [illegible] it did, the amount of spinel or sapphirine was not sufficient to deplete the free silica content substantially.

One sample of symplectite is shown in Figure 32. It consists of an orthopyroxene-sillimanite oriented intergrowth enclosed in anhedral cordierite. Anhedral orthopyroxene and corroded sillimanite occur nearby. Textures do not provide a definite indication of how the symplectites originated; however, several observations appear to be consistent with the occurrence of symplectites:

a) Samples contain abundant quartz (25-30%).

b) Orthopyroxene, garnet and biotite show distinct textures indicative of corrosion and dissolution.

c) Polygonal to lobate areas of cordierite commonly enclose relicts of orthopyroxene, corroded sillimanite (Fig. 33), corroded biotite or symplectites. All these relicts form only 1-3% of the area occupied by cordierite.

These observations suggest that cordierite crystallized as a result of the reaction of high silica activity melt with common mafic minerals. The necessary aluminum was obtained from partial dissolution of sillimanite. Cordierite has locally completely enclosed and isolated remnants of orthopyroxene or sillimanite and preserved them as relicts. Other rarer symplectites may represent isolated silica-depleted residual liquids.

Considering that sillimanite (the least abundant mineral) is still present in thin section, it is assumed that the formation of cordierite had stopped before completion of the reaction. A possible explanation might be a rapid decrease of temperature and increased viscosity of a volatile-starved melt.

Interpretation of the petrological processes from the textural and mineralogical evidence

Additional observations from the well documented profile (Fig. 4 and 5) include;

I. Broken-off sapphirine crystals from the mafic granulite-mobilizate contact and deformed fragments of rocks engulfed in mobilizate (Fig. 34, 35) demonstrate that the mobilizate had a high viscosity.

II. A general lack of hydrous minerals in surrounding rocks (relatively rare khaki-brown hornblende in some layers) and the restriction of phlogopite mainly to the ultramafic

or mafic granulites, indicate that water vapor and other volatiles were scarce.

III. A variety of corona types occur in a single hand specimen or thin section, together with spinel or sapphirine without coronas, suggesting that silica consumption from mobilizate proceeded unevenly and was hampered by slow silica diffusion in a viscose and dry melt. Some crystals and rock fragments could have been engulfed by and reacted quickly with a high silica activity mobilizate, whereas others might be engulfed by already silica-depleted mobilizate and thus be preserved without change; and

IV. Some textures suggest relatively static crystallization (Fig. 30, 31), others (Fig. 35) suggest dynamic conditions.

Chatterjee and Schreyer (1972) investigated experimentally the reaction enstatitess + sillimanite = sapphirine$_{ss}$ + quartz in the system MgO-Al_2O_3-SiO_2 under "dry" conditions. Their temperature pressure diagram shows a univariant curve of low positive slope between 1100°C/14kb and 1400°C/18kb. Considering the relative position of this curve to the others in the schematic temperature pressure grid around I_{13} one must conclude that this reaction brackets the highest pressure conditions.

In a photomicrograph Chatterjee and Schreyer (1972) show sapphirine mantled by a sillimanite-orthopyroxene corona from Wilson Lake, Central Labrador, that is similar to coronas from Sipiwesk Lake (Figs. 22, 23 in this paper). Despite the uncertainty of the combined influence of the iron and possibly a small amount of volatiles, the reaction Spr + Qtz = 2Sil + Opx may represent the upper temperature pressure conditions for these rocks on Sipiwesk Lake.

Deposition of plagioclase overgrowth rims on corona mineral assemblages indicates that the crystallization in the $(Fe,Mg)O$-Al_2O_3-SiO_2 system was completed before crystallization in the $(Na,K)_2O$-CaO-Al_2O_3-SiO_2 system began. Since ferromagnesian minerals, formed simultaneously or later than feldspars, were not observed, it must be concluded that crystallization in both the above mentioned systems did not overlap substantially. The crystallization of plagioclase therefore indicates a lower temperature pressure bracket for crystallization in the $(Mg,Fe)O$-Al_2O_3-SiO_2 system.

Although substantial experimental work has been done on melts of granitic composition, data pertaining to more basic melt compositions are scarce. Textures in Figures 29 to 31 show enclaves of plagioclase (An_{40}) and perthite but no quartz. Thus the assemblage approximates the An-Ab-Or system. According to Yoder et al. (1957), such plagioclase would crystallize above 1050°C at PH_2O = 5kb. Yoder (1970) published an Ab-An diagram of plagioclase-melting up to 10 kb with and without water. It shows that plagioclase An_{40} crystallizes above 1050°C.

In the light of the estimated upper and lower temperature pressure brackets from available experimental work, it is difficult to dismiss the suggestion of Morse and Talley (1971, op. cit.) that metamorphic "conditions in excess of 11 kb, 1100°C and possibly as high as 13 kb, 1150°C" existed in these types of sapphirine bearing granulites. The mineralogical and textural observations of the present study suggest that the Sipiwesk Lake granulites closely approximate the above cited experimental systems and also the granulites from Wilson Lake. Thus the temperature pressure conditions should be similar to those estimated by Morse and Talley (1971, op. cit.).

This estimate, however, was not confirmed by Arima and Barnett (1984) who worked with several samples from the same locality on Sipiwesk Lake. They derived the following metamorphic conditions: 860-890°C and 3.0-11.2 kb for "orthopyroxene-cordierite granulites" and 780-880°C and 9 ± 1 kb for "feldspar-sillimanite granulites". One is aware of extreme complexities and difficulties connected with obtaining reliable thermodynamic data and their calibration (Newton and Perkins, 1982) for petrological calculations. It is understandable that each attempt to derive metamorphic conditions is a difficult task that must be highly commended despite uncertainties and limitations that are part of the method. Some of Arima and Barnett's assumptions and statements do not agree with observations presented in this paper:

1. Their photograph of "orthopyroxene-cordierite" granulite (Fig. 2a, p. 103) shows a fractured Spl-Spr-Opx-Crn-Phl assemblage of the ultramafic granulite **without cordierite**. This may represent a sample torn from the transitional zone between the central (Spl-Phl-Opx-Crn) assemblage and border (Spr-Opx-Crn) zone of ultramafic granulite engulfed in mobilizate. Intense fracturing of the sample would invite penetration of mobilizate resulting in sapphirine transformation into cordierite in proximity to the location of the photograph. Thus cordierite is recorded in their Table 1 under P07.

2. Their photograph of "feldspar-sillimanite" granulite (Fig. 2b, p. 103) is an example of one of the various coronas (sillimanite-garnet) developed in "mobilizate" and/or "mobilizate melange".

3. Their statement that "spinel and corundum are never found in contact with orthopyroxene and cordierite" (p. 103) is not valid (cf. Fig. 6, 10). Figure 36 shows corundum surrounded by cordierite.

4. In the present study cordierite was not observed in the central zone (Phl-Spl-Opx) of the ultramafic granulite. If cordierite is the reactant as suggested by Arima and Barnett (1984), then the reaction: cordierite + spinel = sapphirine + orthopyroxene should consume all primary cordierite in reacting with spinel to produce sapphirine + orthopyroxene, and the mineral assemblage spinel-sapphirine-orthopyroxene should be observed. However, sapphirine is not found in the central zone of ultramafic granulite and thus excludes the presence of primary cordierite.

The contact zones of the ultramafic granulite with mobilizate contains the mineral assemblage sapphirine + orthopyroxene but not spinel and/or primary cordierite. This would require precisely balanced reactants spinel + primary cordierite and therefore contradicts conclusions made for the central zone. Furthermore, the incipient formation of sapphirine can be observed in the transition zone and it does not contain any cordierite. Therefore, it is apparent

that the reaction cordierite + spinel = sapphirine + orthopyroxene cannot be applied to sapphirine bearing granulites at Sipiwesk Lake.

5. It has been shown that cordierite observed in the sapphirine-bearing granulites at the Sipiwesk Lake locality originated in all examined cases as a product of sapphirine reaction with silica in mobilizate. One sample containing symplectites, where cordierite may have been generated from other mafic minerals due to a silica-supersaturated mobilizate is the only exception. Otherwise, sapphirine, orthopyroxene, cordierite, sillimanite, garnet and feldspars are commonly all present in one thin section of the "mobilizate melange". Therefore, the separation of sapphirine-bearing granulites into "orthopyroxene-cordierite" and "feldspar-sillimanite" groups is artificial.

6. No clear textural evidence was presented by Arima and Barnett to support the suggested reaction: sapphirine + garnet + quartz = orthopyroxene + sillimanite involving "a relic" sapphirine "of an earlier stage of metamorphism".

It is apparent that Arima and Barnett applied advanced techniques to the samples for which the mode of origin was assumed and postulated but not investigated. As a result their quantitative petrogenetic conclusions are based on reactions that, according to evidence presented in the present study, could not have occurred in these rocks.

Minerals in possible equilibrium

A crucial requirement for application of thermodynamic calculations is that minerals are in equilibrium (Newton and Perkins, 1982, op.cit.). Textural observations from the Sipiwesk Lake locality yield good definite suggestions of minerals in possible equilibrium at certain metamorphic conditions. These suggestions are displayed in Table 2:

Although it is reasonable to infer that P-T-X[1] metamorphic conditions were likely higher and certainly preceded those designated as [7], [8] and [9], it is not intended to imply by the above list (Table 2) that the P-T-X conditions followed a straight decreasing path from [2] to [6b]. It represents a systematic way of listing reactants of differing alumina content and different products with respect to the activity of silica. The exact P-T-X conditions of these reactions are unknown, but all had occurred after P-T-X[1] had diminished and before P-T-X[7] had arisen.

From the list of mineral assemblages it is apparent that certain P-T-X metamorphic conditions are characterized by no more than two minerals. The only exception is (Spl-Phl-Opx-Crn) assemblage[1]. This indicates that from three or more minerals in mutual contact only one or two are characteristic for certain P-T-X conditions and the rest are metamorphic relicts. The assumption that minerals in mutual contact are usually in equilibrium is unwarranted. Whether or not partial equilibration of some minerals took place under new P-T-X conditions is uncertain. However, it is likely that such a re-equilibration process was considerably hampered under "dry conditions".

TABLE 2
Minerals in Equilibrium under Given P-T-X Conditions

Ultramafic Granulite	Mineral Assemblages	P-T-X
Central zone:	**Spl-Phl-Opx-Crn**	[1]
Outer zone:	*Crn[1], Opx[1], Spl[1]↯, Phl[1]↯,* **Spr-Rt**	[2]
Contact:	*Crn[1], Opx[1], Phl[1], Spl[1]↯,* **Spr-Rt**	[3]
Mobilizate:	*Spr[2]↯*/**Crd** or **Crd-Sil**	[4a]
	Spr[3]↯/**Crd** or **Crd-Sil**	[4b]
	Spr[2]↯/**Sil-Opx** or **Sil-Grt**	[5a]
	Spr[3]↯/**Sil-Opx** or **Sil-Grt**	[5b]
	Spr[2]↯/**Grt**	[6a]
	Spr[3]↯/**Grt**	[6b]
	Pl may be in contact with all mineral assemblages listed above (such as (*Sil-Opx*/**Pl**))	[7]
	Kfs may be in contact with all mineral assemblages listed above (such as (*Spr/Sil-Opx/Pl*/**Kfs**))	[8]
	Qtz may be in contact with all minerals above but not likely with *Spl, Spr or Crn*	[9]

Explanation notes:

Italics [ ]: a mineral was formed at different P-T-X conditions [that are indicated in brackets] and does not react during new P-T-X conditions.

Italics [ ]↯: a mineral was formed at different P-T-X conditions [that are indicated in brackets] and the arrow signifies breakdown under new P-T-X conditions.

Bold print: indicates minerals in equilibrium under given P-T-X conditions.

The first step for petrogenetic calculations is to isolate minerals that were in equilibrium under certain P-T-X conditions (cf. list above) and to investigate their crystallochemical parameters with respect to the others to check for re-equilibration. The textural observations presented in this paper offer such a starting point.

CONCLUSIONS

Lithological and textural investigations of the granulite rocks at the Sipiwesk Lake locality established that:

1. Sapphirine originated only in rocks that contained spinel and that were intruded by mobilizate of sufficient silica activity. Sapphirine occurrence is limited to the vicinity of the contact between the spinel-bearing ultramafic layer and mobilizate.

2. Cordierite is secondary and originated from sapphirine or, in one case, from other mafic minerals in reactions dependent upon the degree of silica activity of the mobilizate.

3. Many mineral phases are observed to be in mutual contact; however, the reactants that produced the variety of mineralogical corona types are only two: sapphirine and free silica in mobilizate. Other minerals appear to remain passive.

4. Where sapphirine was exhausted or never present, other mafic minerals have may reacted with silica-rich mobilizate to produce cordierite.

5. One or two minerals originated during certain P-T-X conditions and thus was (were) equilibrated under given metamorphic conditions because there were only two reactants involved at the time. Other minerals may be passive relicts of previous metamorphic conditions and thus unequilibrated.

6. Current metamorphic grids that have been constructed from a set of reactions, assuming involvement of all observed phases in the rock, may not directly apply to corona-forming reactions in the granulites at Sipiwesk Lake.

7. Mineral assemblages listed in Table 2 could serve as a logically justified starting point for a detailed crystallochemical investigation and petrological modeling.

8. The P-T-X conditions for formation of coronas could perhaps be derived through experiments closely resembling the suggested chemical reactions.

REFERENCES

Arima M. and Barnett, R.L.
1984: Sapphirine-bearing granulites from the Sipiwesk Lake area of the later Archean Pikwitonei granulite terrain, Manitoba; Contributions to Mineralogy and Petrology, v. 88, p. 102-112.

Chatterjee, N.D. and Schreyer, W.
1972: The reaction enstatite + sillimanite = sapphirine$_{ss}$ + quartz in the system MgO-Al_2O_3-SiO_2; Contributions to Mineralogy and Petrology, v. 36, p. 49-62.

Hubregtse, J.J.M.W.
1980: The Archean Pikwitonei granulite domain and its position at the margin of the northwestern Superior Province (central Manitoba); Manitoba Energy and Mines, Geological Paper GP80-3, 16 p.
1978: Sipiwesk Lake-Landing Lake-Wintering Lake area; In Manitoba Mines, Resources and Environmental Management, Mineral Resources Division, Report of Field Activities, 1978, p.54-62.

Mohan, A., Ackermand, D., Lal, R.K.
1986: Reaction textures and P-T-X trajectory in the sapphirine-spinel-bearing granulites from Ganguvarpatti, Southern India; Neues Jahrbuch Mineralogische Abhandlungen, v. 154, p. 1-14.

Morse, S.A. and Talley, J.H.
1971: Sapphirine reactions in deep-seated granulites near Wilson Lake, Central Labrador, Canada; Earth and Planetary Science Letters, v. 10, p. 325-328.

Newton, R.C. and Perkins III, D.
1982: Thermodynamic calibration of geobarometers based on the assemblages garnet-plagioclase-orthopyroxene (clinopyroxene)-quartz; American Mineralogist, v. 67, p. 203-222.

Robertson, I.D.M.
1977: Some granulite facies metasediments of the Rhodesian part of the north marginal zone of the Limpopo Mobile Belt; In Proceedings of Republic of Botswana, Geological Survey Department Bulletin 12, a seminar pertaining to the Limpopo Mobile Belt, Section Three, p. 157-176.

Yoder, H.S.
1970: Experimental studies bearing on the origin of anorthosite; Geophysical Laboratory, Carnegie Institute of Washington, New York State Museum and Science Service Memoir 18, Paper No. 1562, p. 13-22.

Yoder, H.S., Stewart, D.B. and Smith, J.R.
1957: Ternary feldspars; Carnegie Institute of Washington, Yearbook 56; p. 206-214.

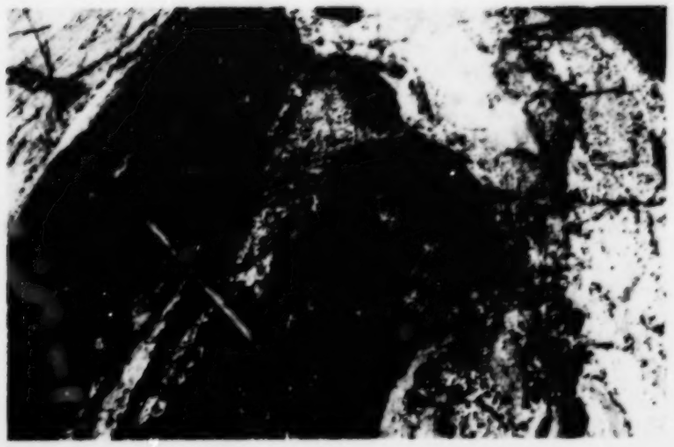

Figure 1: A boudinaged end of disrupted layered ultramafic-mafic granulite intruded by leucocratic mobilizate.

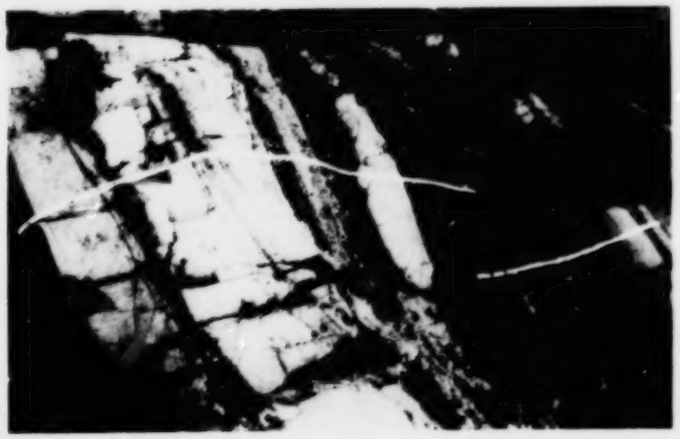

Figure 2: Layered felsic to mafic granulite sequence locally severely tectonized and intruded by leucocratic mobilizate. Medical tape is 2.5 cm wide.

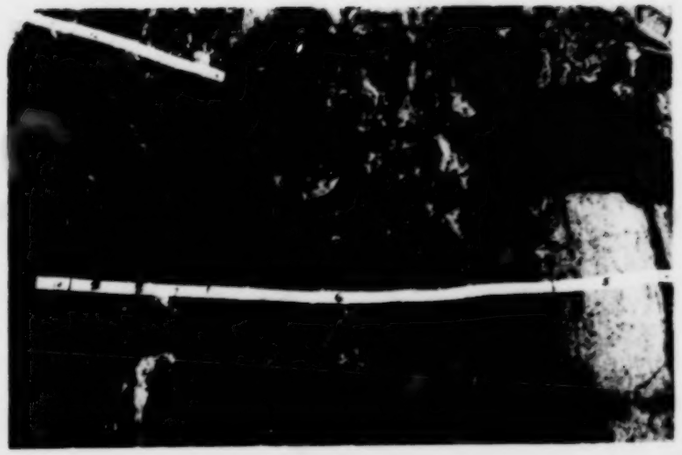

Figure 3: Leucocratic mobilizate carrying numerous ultramafic to felsic fragments. Such chaotically mixed rock is termed "mobilizate melange". The medical tape is 2.5 cm wide and displays reference numbering.

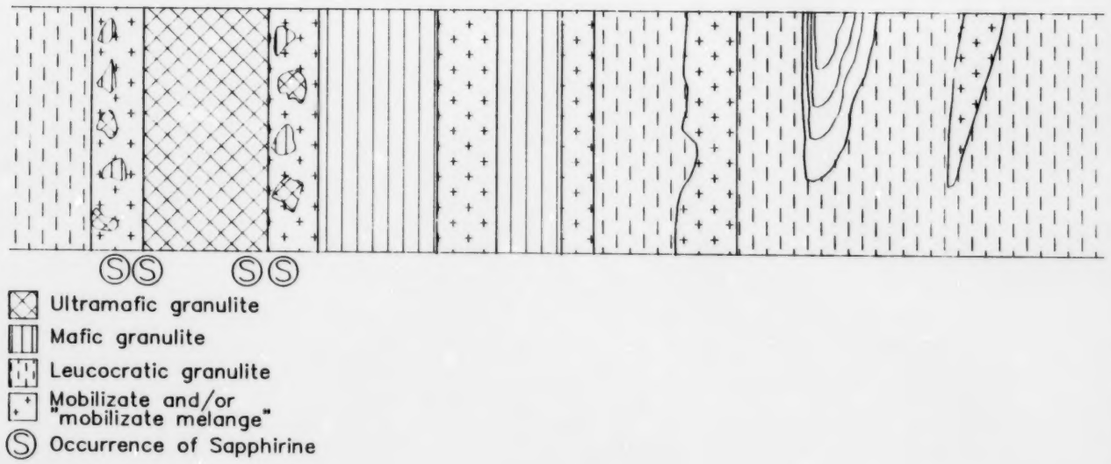

Figure 4: Schematized geological relationships of common principal lithological units.

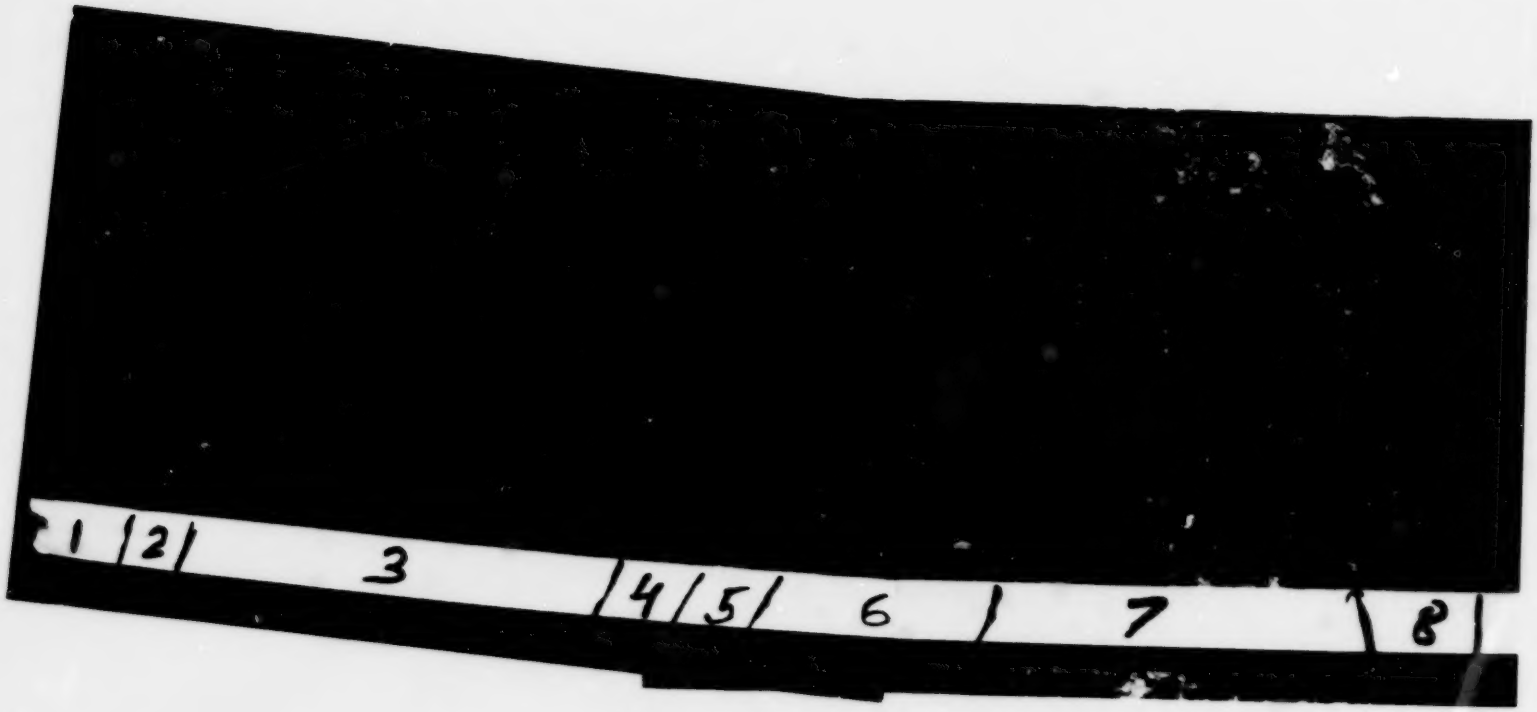

Figure 5: Phlogopite-spinel-orthopyroxene granulite, the most basic rock in the area (marked on the medical tape as 3). Photograph displays area with minimal tectonic disturbance. Note dark elongated clots of spinel which are absent in symmetrical zones 2 and 4. In those the spinel is replaced by sapphirine.

Figure 6: Lepidogranoblastic texture of phlogopite-spinel-orthopyroxene granulite. Note elongated corundum enclosed in the marked orthopyroxene. Plane polarized light. Photograph dimensions: 2 x 3 mm.

Figure 7: Rutile needles enclosed in [001], [010] and [011] directions of orthopyroxene. Crossed nicols. Photograph dimensions: 0.2 x 0.3 mm.

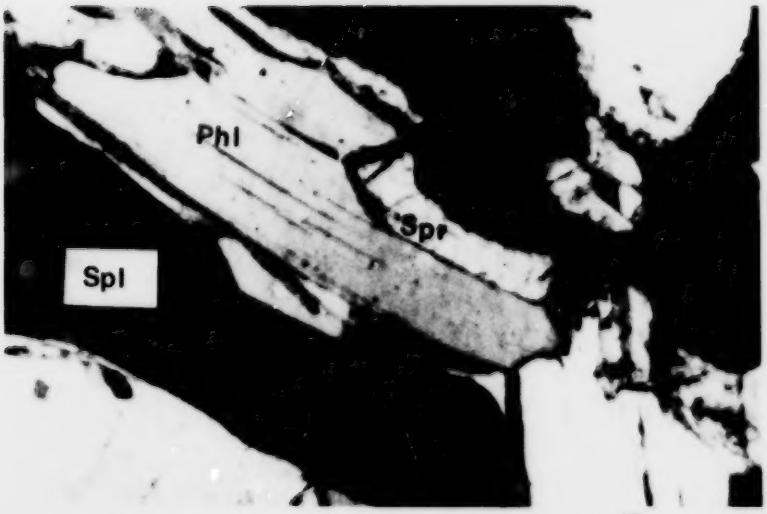

Figure 8: Incipient formation of sapphirine between phlogopite and spinel. Plane polarized light. Photograph dimensions: 0.5 x 0.8 mm.

Figure 9: Sapphirine formation from spinel and phlogopite. Phlogopite is distinctly corroded. Plane polarized light. Photograph dimensions: 0.5 x 0.8 mm.

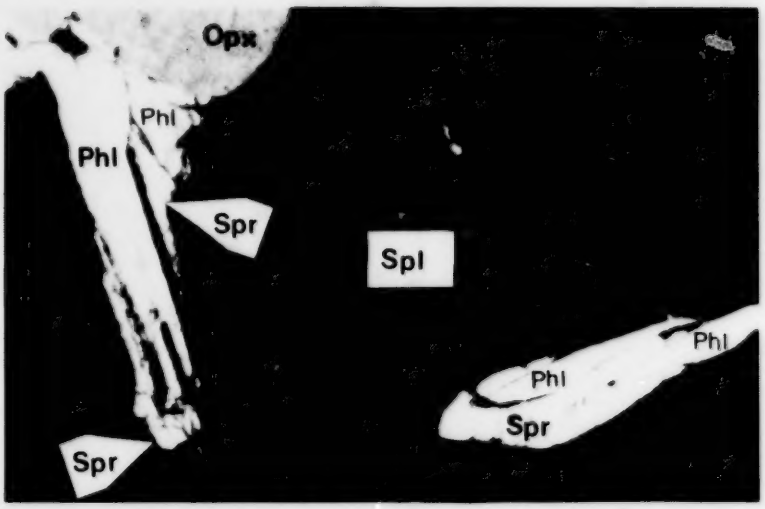

Figure 10: Incipient formation of sapphirine from spinel and phlogopite. Note inert contact between orthopyroxene and spinel. Crossed nicols. Photograph dimensions: 0.5 x 0.8 mm.

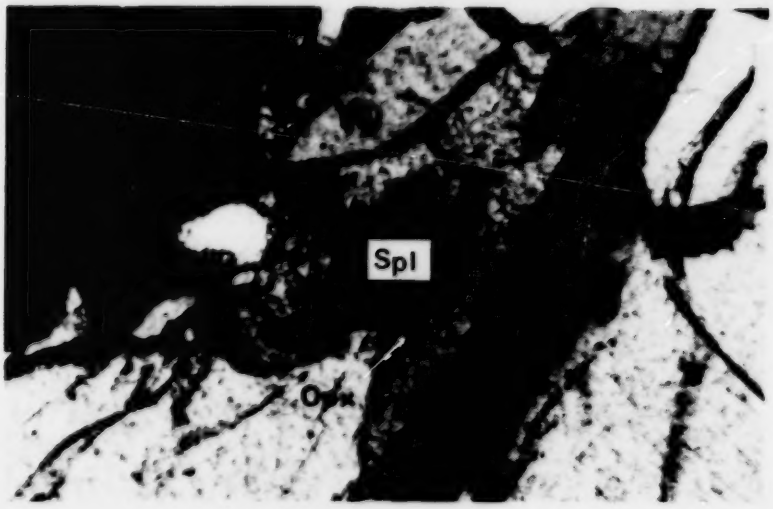

Figure 11: Formation of sapphirine from spinel and phlogopite. Plane polarized light. Photograph dimensions: 0.5 x 0.8 mm.

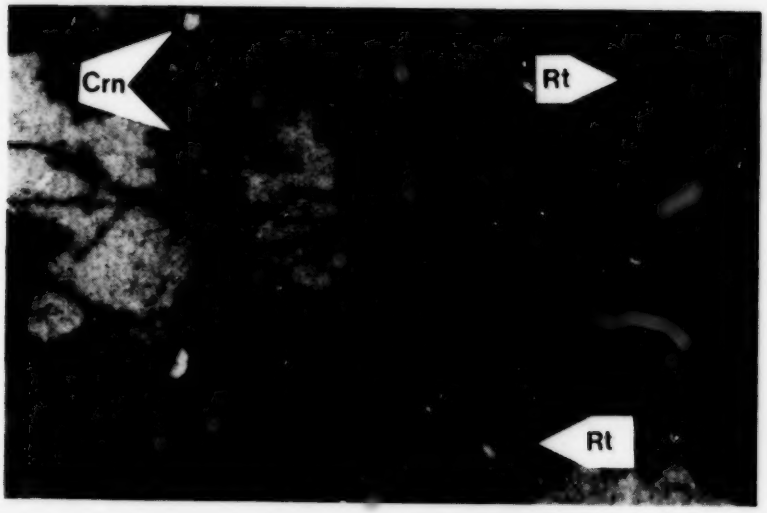

Figure 12: Granoblastic texture of phlogopite-sapphirine-orthopyroxene granulite. All spinel is replaced by anhedral sapphirine. The modal content and the crystal size of phlogopite is greatly reduced. Rutile forms discrete crystals. Plane polarized light. Photograph dimensions: 2 x 3 mm.

Figure 13: Areas of plagioclase and cordierite represent embayments originally filled with mobilizate. Note abundance and size of phlogopite laths directly on the contact. Plane polarized light. Photograph dimensions: 2 x 3 mm.

Figure 14: Mobilizate-ultramafic granulite contact. Note difference in sapphirine crystal shape and size (outlined in black) directly on the contact and away from it. Phlogopite is almost absent away from the contact. Plane polarized light. Photograph dimensions: 5 x 8 mm.

Figure 15: Subhedral crystal of sapphirine "broken off" the contact between ultramafic granulite and mobilizate. Plane polarized light. Photograph dimensions: 5 x 8 mm.

Figure 16: Quartz in mobilizate 15-25 cm away from the ultramafic granulite. Crossed nicols. Photograph dimensions: 2 x 3 mm.

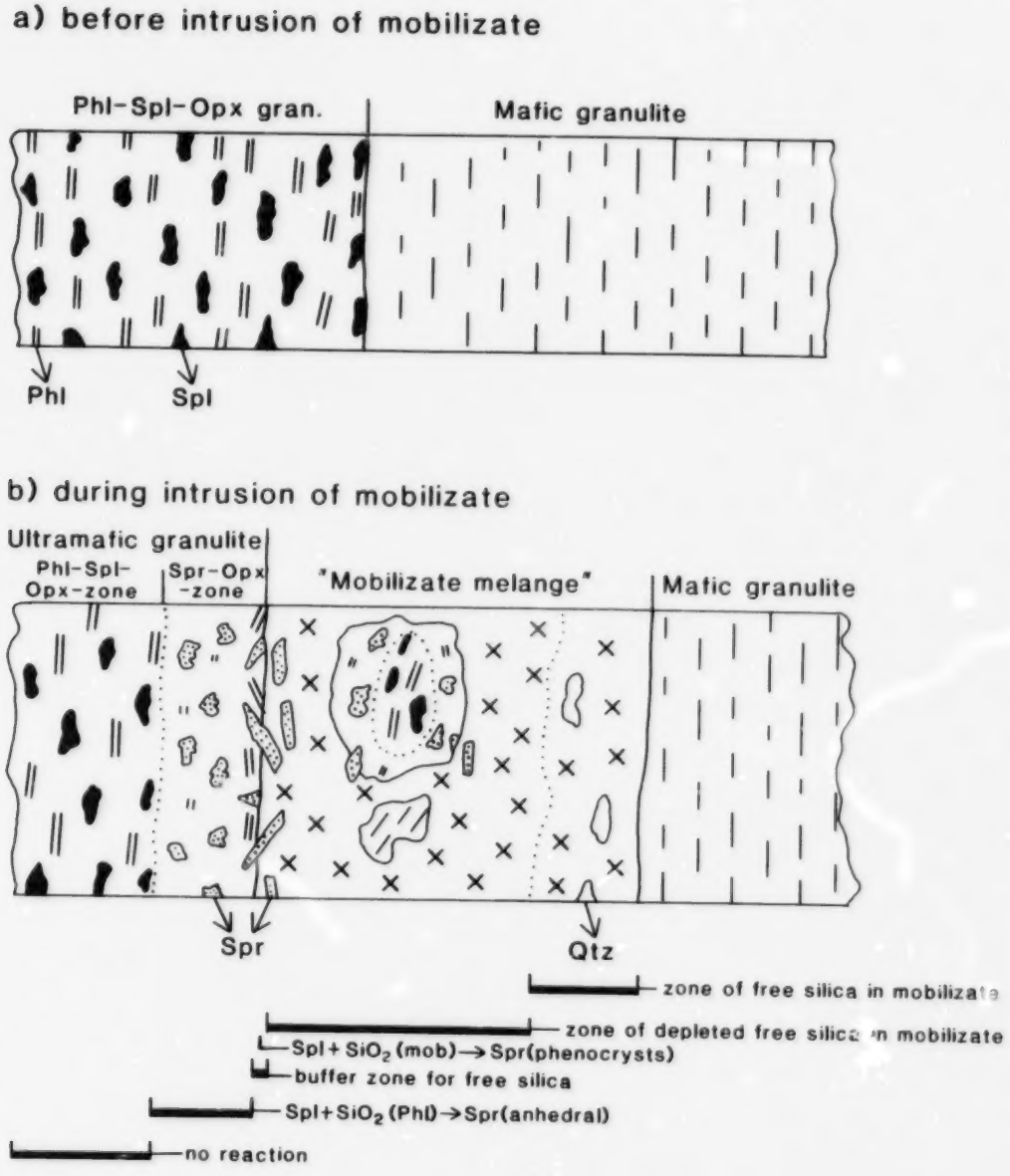

Figure 17: a) Contact between ultramafic (phlogopite-spinel-orthopyroxene) granulite and mafic granulite before intrusion of mobilizate.

b) Mobilizate which contained free silica intruded along the contact of the ultramafic-mafic pair and reacted with the exposed spinel to form phenocrysts of sapphirine and simultaneously preserving phlogopite. Marginal zone of the ultramafic granulite received sufficient heat (activation) energy but no free silica. As a result, silica was pirated from phlogopite to form anhedral sapphirine from spinel. During intrusion accompanied by tectonism various rock fragments were incorporated into mobilizate resulting in "mobilizate melange". Relatively narrow zone of phlogopite-sapphirine-orthopyroxene granulite may indicate rapid cooling of the intruding mobilizate.

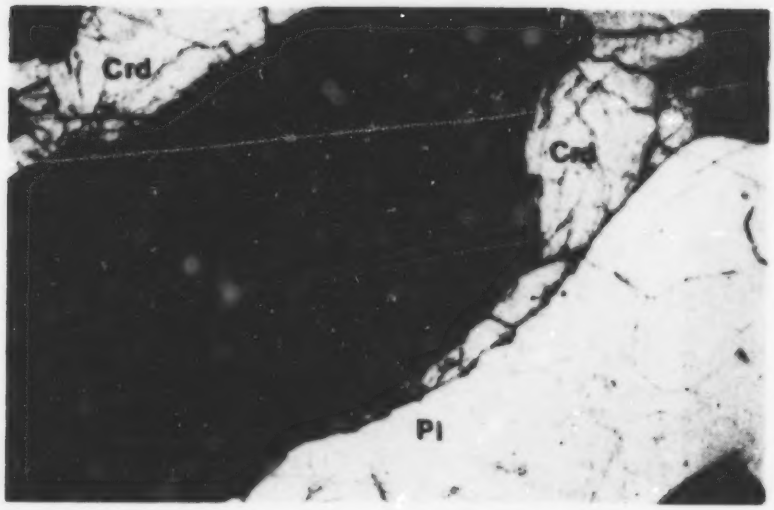

Figure 18: Incomplete rim of cordierite around sapphirine crystal. Plane polarized light. Photograph dimensions: 2 x 3 mm.

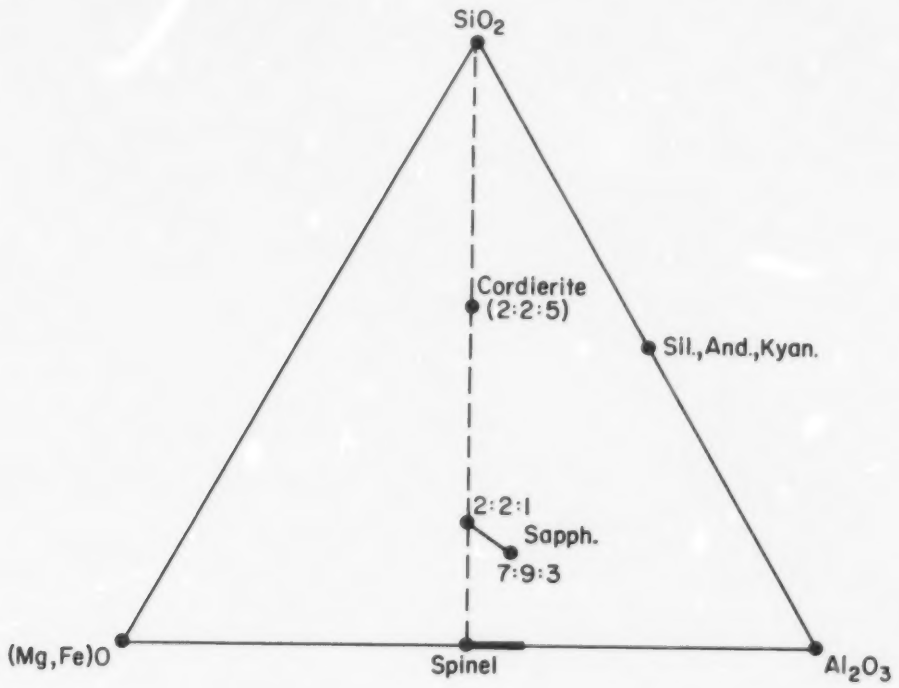

Figure 19: Graphical relationship among spinel, sapphirine, cordierite and sillimanite in the SiO_2-(Mg, Fe)O-Al_2O_3 system.

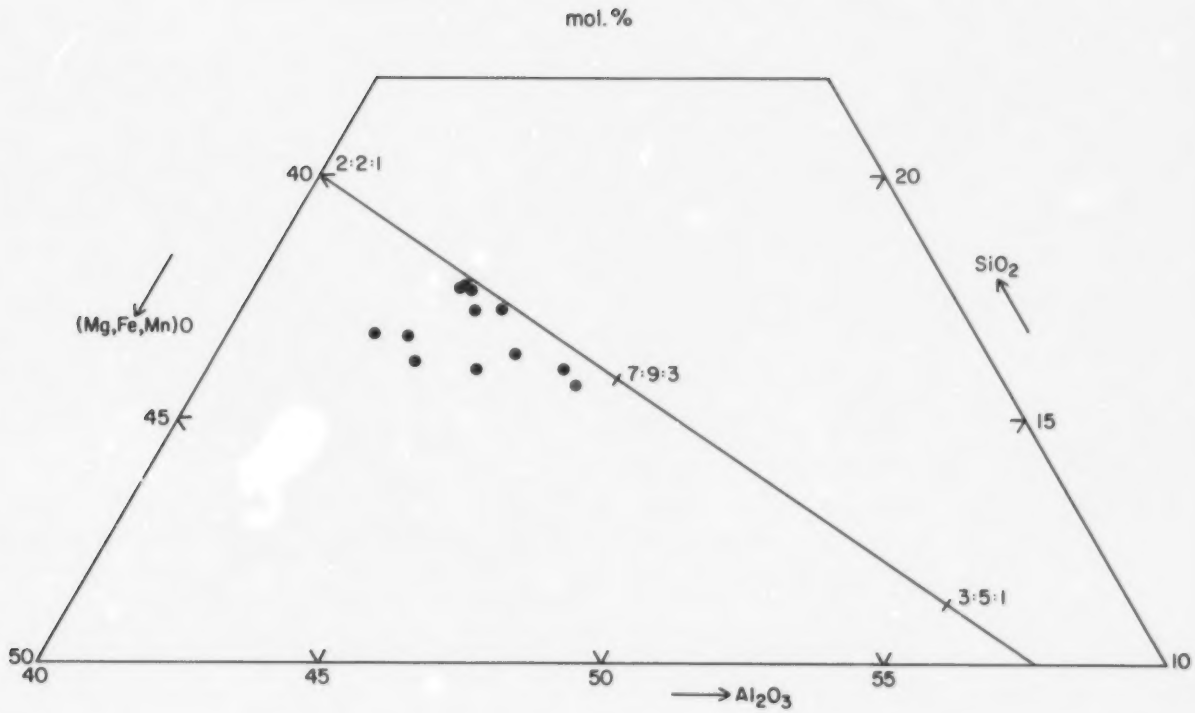

Figure 20: Plot of the sapphirine compositions.

Figure 21: Sillimanite-cordierite corona. Plane polarized light. Photograph dimensions: 0.5 x 0.8 mm.

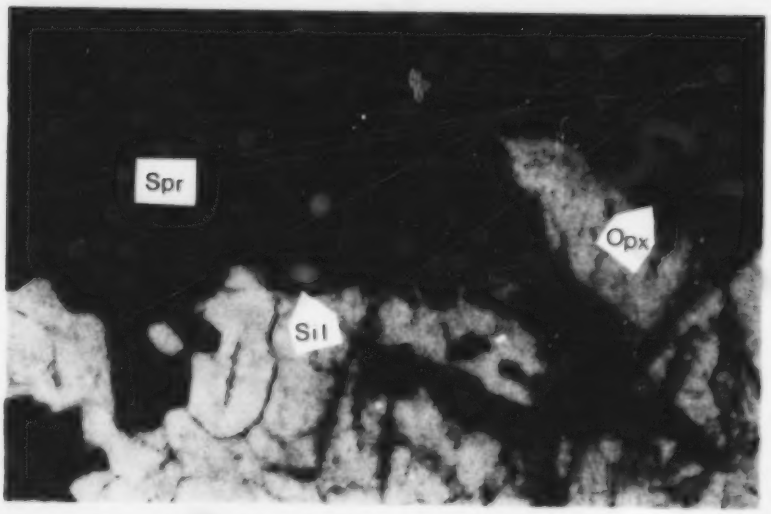

Figure 22: Sillimanite-orthopyroxene corona. Sillimanite rim consists of few mono-crystals. Plane polarized light. Photograph dimensions: 2 x 3 mm.

Figure 23: Sillimanite-orthopyroxene corona. Plane polarized light. Photograph dimensions: 0.5 x 0.8 mm.

a)

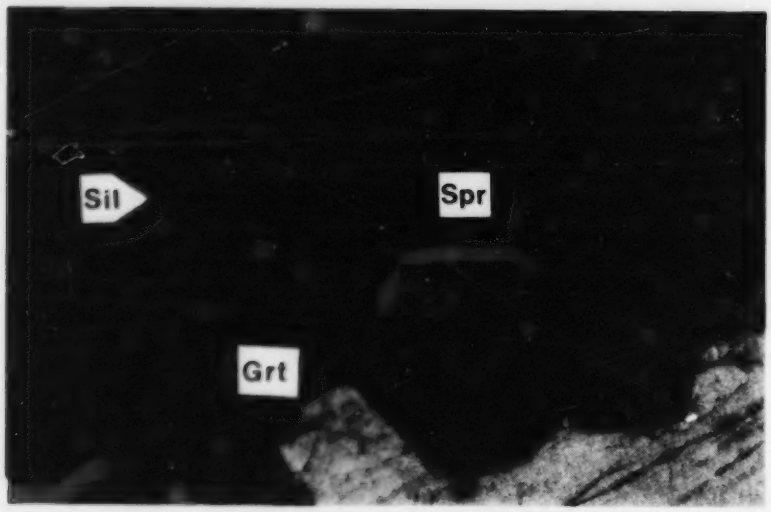

b)

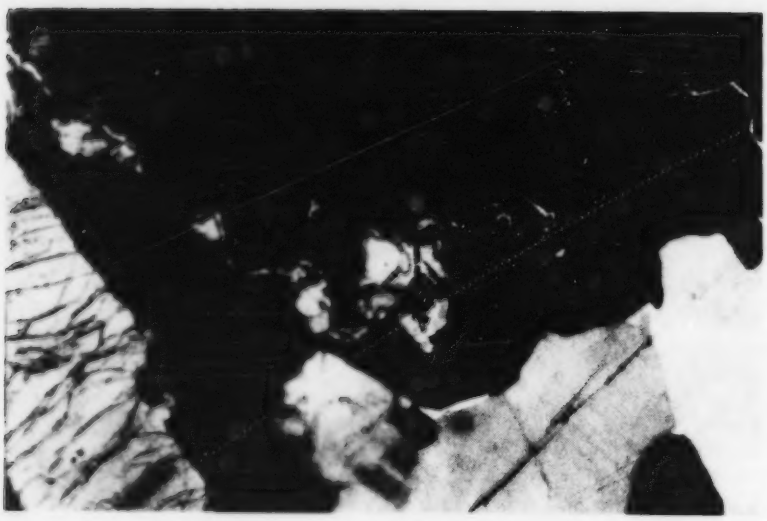

Figure 24: a) Sillimanite-garnet corona. Plane polarized light.
b) Same object in crossed nicols. Photograph dimensions: 2 x 3 mm.

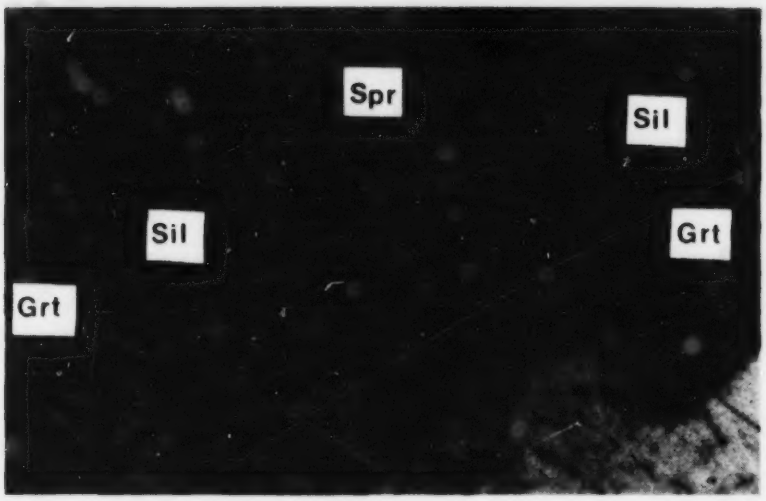

Figure 25: Sillimanite-garnet corona. Plane polarized light. Photograph dimensions: 2 x 3 mm.

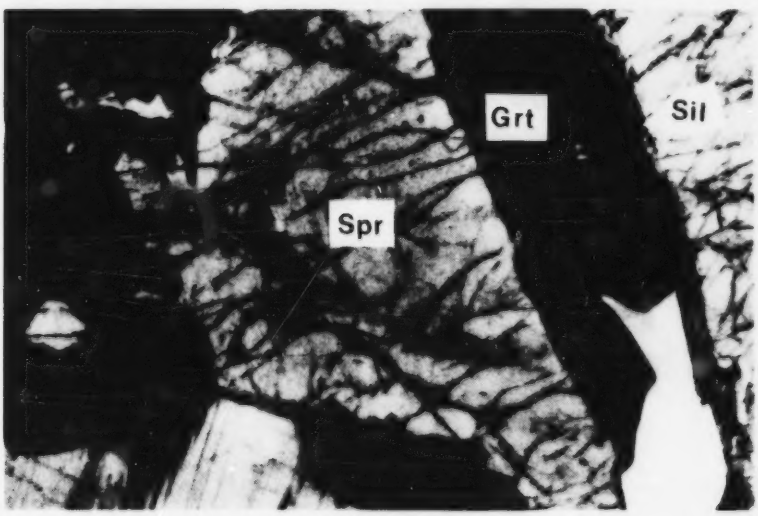

Figure 26: Garnet formation from sapphirine (centre and left). Crossed nicols. Photograph dimensions: 2 x 3 mm.

Figure 27: Spinel (black) overgrown by garnet or enclosed by plagioclase. Plane polarized light. Photograph dimensions: 2 x 3 mm.

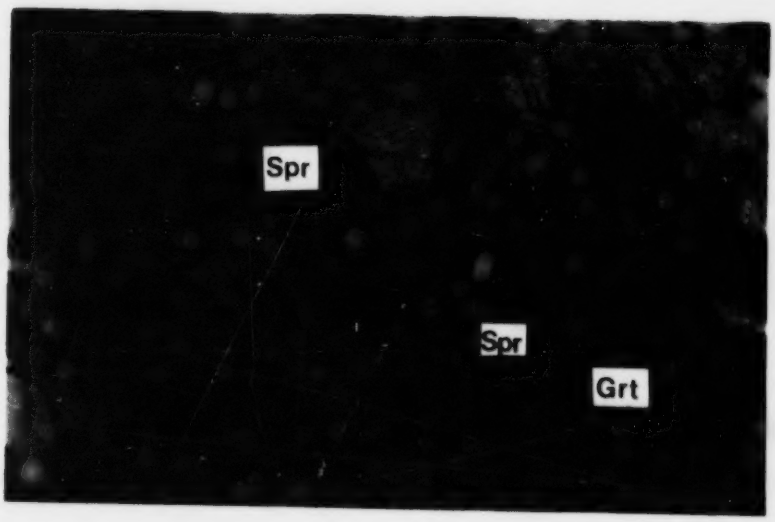

Figure 28: Sapphirine enclosed in plagioclase and/or garnet. Plane polarized light. Photograph dimensions: 2 x 3 mm.

Figure 29: Sapphirine rimmed by cordierite corona serves as crystallization centre for subsequent crystallization of minerals in the $(Na,K)_2O$-CaO-Al_2O_3-SiO_2 system: plagioclase and potassium feldspar. Plane polarized light. Photograph dimensions: 0.5 x 0.8 mm

Figure 30: Relicts of two sapphirine crystals rimmed by cordierite coronas are mantled by plagioclase. Perthite crystallized as the last mineral. Plane polarized light. Photograph dimensions: 0.2 x 0.3 mm.

Figure 31: Symmetrical mineral zoning around sapphirine crystal relics (dark). Plane polarized light. Photograph dimensions: 0.2 x 0.3 mm.

Figure 32: Orthopyroxene-sillimanite symplectite enclosed in cordierite. Plane polarized light. Photograph dimensions: 0.2 x 0.3 mm.

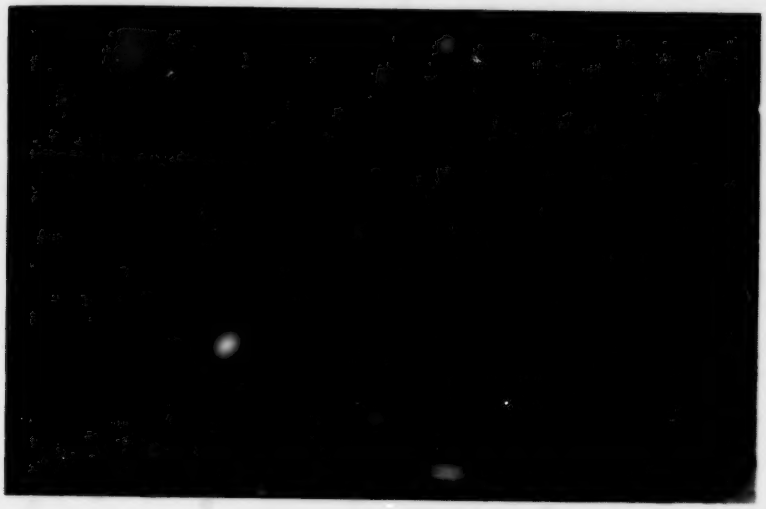

Figure 33: Ornamental relict of sillimanite enclosed in cordierite and resembling symplectite. Corrosion is inferred to be responsible for this ornamental shape since in several similar instances the continuity of fractures could be observed despite the extensive unfractured embayments. Photograph dimensions: 0.2 x 0.3 mm.

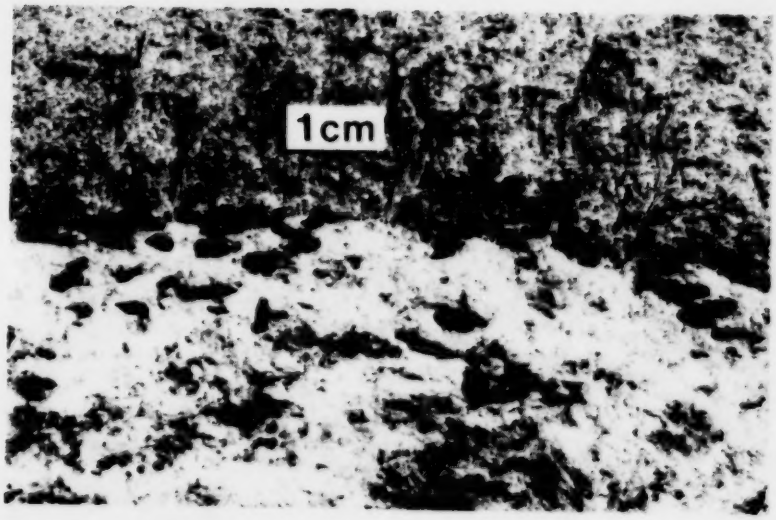

Figure 34: Contact of sapphirine orthopyroxenite with mobilizate. Note numerous sapphirine phenocrysts (emphasized by black ink) on contact or detached crystals in the vicinity of contact.

Figure 35: Elongate and deformed spinel orthopyroxenite fragments with a distinct reaction rim floating among other rock fragments in "mobilizate melange". Width of medical tape is 2.5 cm.

Figure 36: Corundum grain surrounded by cordierite.

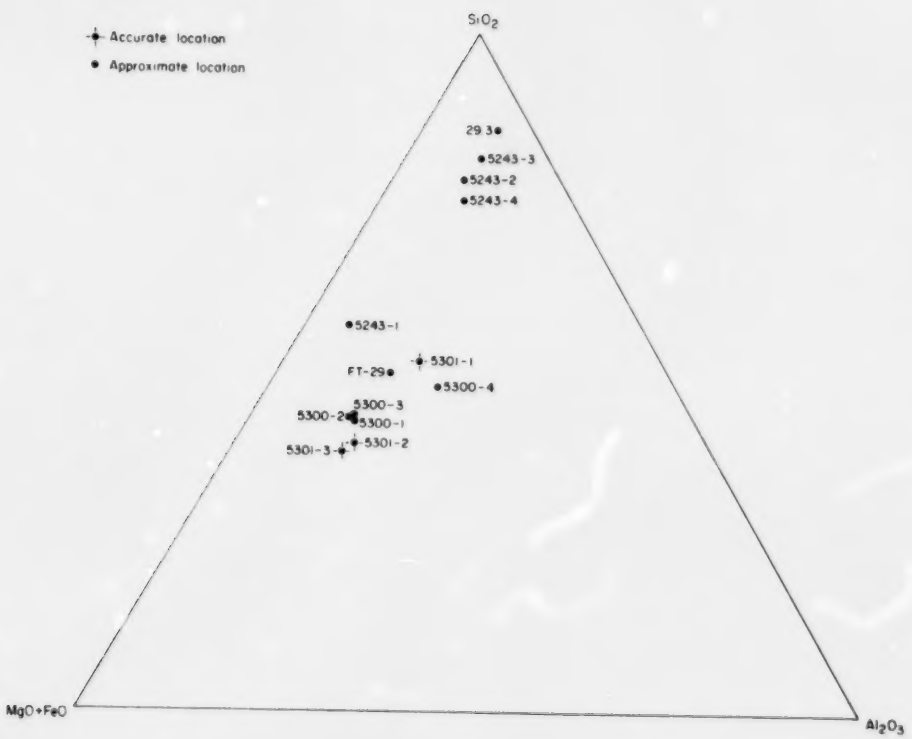

Figure 37: Plot of all chemical analyses in the SiO_2-(Mg,Fe)O-Al_2O_3 diagram (in Appendix A).

APPENDIX A

Whole Rock Chemical Analyses

List of the Analyzed Rocks:

Sample No.	Rock Name
5301-3	Phlogopite-spinel-orthopyroxene granulite
5301-2	Rutile-sapphirine-orthopyroxene granulite
5301-1	Mobilizate near the ultramafic layer
5300-1	Phlogopite-sapphirine-spinel-orthopyroxene granulite
5300-2	Phlogopite-sapphirine-spinel-orthopyroxene granulite
5300-3	Phlogopite-cordierite-sapphirine granulite
5300-4	Potash feldspar-phlogopite-sapphirine granulite
FT-1-29	"mobilizate melange"
5243-1	Phlogopite-plagioclase-clinopyroxene-orthopyroxene granulite
5243-2	Orthopyroxene-cordierite-quartz granulite
5243-3	Orthopyroxene-cordierite-quartz granulite
FT-1-29-3	Garnet-plagioclase-quartz granulite

Chemical analyses 5301-3, 5301-2 and 5301-1 correspond to zones 3, 4 (or 2) and 5 (or 1) on Figure 5, respectively.

Sample Number	5301-3	5301-2	5301-1	5300-1	5300-2	5300-3	5300-4
Location	Accurate	Accurate	Accurate	Approx.	Approx.	Approx.	Approx.
Major minerals	Opx,Spl, Phl	Opx,Spr, Rt	Pl,Spr, Crd,Opx	Opx,Spl, Spr,Phl	Opx,Spl, Spr,Phl	Spr,Crd, Phl	Spr,Phl, Kfs
SiO_2 (weight %)	36.85	38.85	46.45	41.95	42.95	43.3	40.75
Al_2O_3	23.17	25.17	26.24	23.33	21.87	23.03	31.42
Fe_2O_3	3.76	2.32	1.35	1.38	1.64	1.45	1.83
FeO	7.63	7.76	5.44	5.72	5.6	5.68	2.28
CaO	0.3	0.25	2.25	0.53	0.27	0.44	0.18
MgO	24.68	24.35	14.82	24.96	25.51	24.68	15.26
Na_2O	0.09	0.05	1.53	0.12	0.08	0.07	1.06
K_2O	1.94	0.3	0.62	0.3	0.41	0.17	5.18
TiO_2	0.77	0.79	0.97	0.16	0.17	0.18	0.26
P_2O_5	0.24	0.17	0.12	0.07	0.04	0.03	0.02
MnO	0.06	0.07	0.07	0.06	0.07	0.07	0.07
NiO	0	0	0	0	0	0	0
Cr_2O_3	0	0	0	0	0	0	0
H_2O	0.71	0.33	0.45	0.87	1.07	0.64	0.9
S	0	0	0	0.01	0	0.01	0
CO_2	0.05	0.07	0.45	0.63	0.37	0.64	0.12
Total	100.25	100.48	100.76	100.09	100.05	100.39	99.33
Cu (ppm)	4	6	19	6	5	5	6
Ni	17	28	54				4
Zn	219	104	108	121	126	139	75
Pb							12
Rb	108	62	32	34	44	28	482
Ba	240	380	550	180	140	90	510
Sr	10	5	60	10	10	10	20
Cr	13	18	13	4			

Sample Number	FT-1-29	5243-1	5243-2	5243-3	5243-4	FT-1-29-3
Location	Approx.	Approx.	Approx.	Approx.	Approx.	Approx.
Major minerals	Crd,Opx	Opx,Cpx, Pl,Phl	Qtz,Crd, Opx	Qtz,Crd, Opx	Pl,Qtz, Opx	Qtz,Pl, Grt
SiO_2 (weight %)	49.55	51	71.75	74.1	64.2	74.15
Al_2O_3	22.55	8.7	14.07	14.94	15.57	14.63
Fe_2O_3	0.77	1.01	0.69	0.36	0.9	0.47
FeO	7.59	7.68	3.66	1.96	4.48	1.9
CaO	0.18	12.16	0.99	1.2	5.85	3.6
MgO	17.36	17.84	5.42	3.9	4.92	1.3
Na_2O	0.29	0.39	1.39	1.67	2.11	3.15
K2O	0.19	0.21	0.68	0.82	0.7	0.54
TiO_2	0.3	0.24	0.17	0.15	0.42	0.04
P_2O_5	0.05	0.74	0.02	0.01	0.05	0.02
MnO	0.12	0.23	0.06	0.03	0.11	0.07
NiO	0	0	0	0	0	0
Cr_2O_3	0	0	0	0	0	0
H_2O	0.66	0.27	0.26	0.31	0.13	0.24
S	0.02	0	0.02	0	0	0
CO_2	1	0.1	0.24	0.37	0.08	0.05
Total	100.63	100.57	99.42	99.82	99.52	100.15
Cu (ppm)	18	2	64	13	2	2
Ni	15	560	6		58	
Zn	149	140	147	78	88	25
Pb					2	12
Rb	39	2	18	24	26	8
Ba	55	130	310	430	520	520
Sr	15	30	105	135	300	210
Cr	18	860			197	4

APPENDIX B

Mineral Microprobe Analyses

Notes:

Minerals identified for microprobe analysis in polished thin sections were chosen in an early phase of the investigation. The primary concern was to provide documentation of the mineral paragenesis. Mutual contacts of minerals in a given paragenesis was the other criterion for selection. However, in light of textural observations made later and presented in this paper, both traditional selection criteria now appear to be too crude and perhaps insufficient. Thus the analyses presented below are perhaps of documentary value only.

Samples 5301-3, 5301-2 and 5301-1 correspond to zones 3, 4(or 2) and 5 (or 1) on Figure 5, respectively.

Polished thin section (I) could not be matched with the original hand specimen and is designated by ?. The sample is part of "mobilizate melange".

The meaning of the "location code" is as follows:

The capital letter designates a particular polished thin section. The first number after the capital letter (separated by dash) designates a location number of a (considered) mineral occurrence.

The second number (separated from the first by a slash) designates the number assigned to a particular mineral in a given paragneiss. Polished thin sections and detailed photographs of analyzed grains are stored with the author.

Mineral analyses are arranged in the following order: spinel, sapphirine, orthopyroxene, clinopyroxene, phlogopite, cordierite, garnet, plagioclase, potassium feldspar, sillimanite, rutile, hornblende, apatite, ilmenite, magnetite, vermiculite, pyrite and chalcopyrite.

Spinel

Sample Number Location	5301-2 B-1/1	5301-2 B-1/2	5243-2 E-1/2
SiO_2 (wt %)	0.13	0.13	0.71
TiO_2	0.01	0.04	0.01
Al_2O_3	66.71	66.67	54.12
FeO	16.95	16.98	19.86
MnO	0.09	0.06	0.02
MgO	17.03	17.20	8.44
CaO	0.02	0.01	0.01
Na_2O			
K_2O			0.02
ZnO	0.23	0.21	
BaO			Cr 5.60
P_2O_5			
			Zn 9.53
Total	101.18	101.29	98.32
Atoms			
Si	0.020	0.020	0.121
Ti	0.001	0.004	0.002
Al	11.940	11.918	10.934
Fe	2.152	2.153	2.847
Mn	0.012	0.008	0.003
Mg	3.854	3.888	2.157
Ca	0.004	0.001	0.001
Na			
K			0.004
Zn	0.026	0.023	1.206
Ba			Cr 0.758
P			
Oxygens	24.000	24.000	24.000

Sapphirine

Sample	**5301-2**	**5301-2**	**5301-1**	**5301-1**	**5301-1**	**5243-4**
Location	**B-1/4**	**B-2/3**	**B-4/2**	**A-2/1**	**A-3/1**	**F-1/1**
SiO2 (wt %)	13.64	13.06	13.42	13.72	13.65	12.85
TiO2	0.12	0.25	0.05	0.08	0.07	0.04
Al2O3	58.97	59.89	58.85	59.85	60.00	60.42
FeO	7.27	6.53	7.08	7.22	7.84	8.35
MnO	0.04	0.06	0.07	0.03	0.08	0.08
MgO	18.11	18.15	17.56	16.64	15.85	15.49
CaO	0.08	0.02	0.29	0.00	0.02	
Na2O				0.05	0.05	0.04
K2O				0.02	0.03	0.01
ZnO		0.03		0.01		0.04
Cu2O3				0.17	0.17	0.10
Total	98.23	97.98	97.31	97.78	97.76	97.41
Atoms						
Si	1.985	1.900	1.971	2.001	1.998	1.893
Ti	0.013	0.027	0.005	0.009	0.007	0.004
Al	10.116	10.268	10.187	10.292	10.348	10.492
Fe	0.885	0.795	0.864	0.881	0.959	1.029
Mn	0.040	0.008	0.008	0.004	0.010	0.010
Mg	3.929	3.936	3.844	3.620	3.457	3.403
Ca	0.012	0.003	0.045		0.003	
Na				0.013	0.013	0.011
K				0.004	0.006	0.002
Zn		0.003		0.001		0.004
Cr				0.019	0.019	0.011
Oxygens	24.000	24.000	24.000	24.000	24.000	24.000

Sample	**?**	**5300-4**	**5300-4**	**5303**	**5303**	**5303**
Location	**I-2/1**	**C-1/1**	**C-2/2**	**D-2/1**	**D-3/3**	**D-4/1**
SiO2 (wt %)	12.57	13.11	12.71	14.13	14.13	14.14
TiO2	0.08	0.01		0.04	0.07	0.07
Al2O3	59.46	64.28	64.26	59.30	59.20	59.80
FeO	7.33	3.77	3.95	8.46	8.27	7.73
MnO	0.15	0.00		0.06	0.07	0.10
MgO	16.41	18.56	18.20	15.85	15.94	16.36
CaO		0.02		0.05	0.03	0.01
Na2O		0.07	0.07	0.12	0.06	0.09
K2O	0.04	0.04	0.04	0.01		0.01
ZnO		0.03	0.01		0.01	0.06
Cu2O3	0.06			0.52	0.55	0.26
Total	96.09	99.9	99.24	98.54	98.34	98.61
Atoms						
Si	1.872	1.841	1.799	2.060	2.061	2.051
Ti	0.009	0.001		0.004	0.008	0.007
Al	10.436	10.644	10.721	10.166	10.180	10.223
Fe	0.913	0.443	0.467	1.031	1.009	0.938
Mn	0.019			0.007	0.009	0.012
Mg	3.641	3.886		3.443	3.467	3.537
Ca		0.003	3.839	0.007	0.004	0.002
Na		0.020		0.013	0.007	0.009
K	0.007	0.007	0.020	0.002		0.003
Zn		0.003	0.007		0.003	0.006
Cr	0.007		0.001	0.060	0.063	0.030
Oxygens	24.000	24.000	24.000	24.000	24.000	24.000

Orthopyroxene

Sample	5301-2	5301-2	5301-1	5301-1	5301-1	5243-4	5243-4	?	?
Location	B-1/5	B-2/2	B-4/4	A-1/1	A-3/4	F-1/2	F-2/3	I-1/2	I-2/4
SiO_2 (wt %)	51.61	52.19	51.22	51.06	49.84	49.23	51.59	50.33	50.51
TiO_2	0.18	0.08	0.12	0.13	0.12	0.13	0.06	0.07	0.06
Al_2O_3	6.07	6.09	7.47	7.21	7.43	8.31	6.88	7.70	8.63
FeO	12.76	13.00	13.90	14.60	16.68	17.73	16.67	16.26	14.28
MnO	0.14	0.12	0.12	0.20	0.19	0.32	0.18	0.46	0.42
MgO	27.55	27.67	26.68	25.62	23.77	23.07	25.06	24.77	25.63
CaO	0.16	0.12	0.15	0.07	0.04	0.04	0.02	0.05	0.05
Na_2O				0.08	0.08	0.05	0.05	0.01	
K_2O				0.02	0.05		0.02		0.02
ZnO	0.03	0.03	0.08	0.02	0.04	0.04	0.02	0.04	0.02
Cr_2O_3					0.11	0.02		0.01	
Total	98.5	99.3	99.75	99.02	98.36	98.96	100.55	99.69	99.61
Atoms									
Si	7.450	7.470	7.337	7.390	7.345	7.251	7.416	7.304	7.261
Ti	0.019	0.009	0.013	0.014	0.013	0.014	0.006	0.008	0.007
Al	1.032	1.027	1.262	1.230	1.290	1.441	1.165	1.316	1.463
Fe	1.540	1.556	1.665	1.768	2.056	2.183	2.004	1.974	1.717
Mn	0.017	0.015	0.015	0.025	0.024	0.040	0.022	0.056	0.051
Mg	5.928	5.906	5.697	5.528	5.222	5.062	5.369	5.358	5.492
Ca	0.025	0.019	0.023	0.011	0.007	0.006	0.003	0.007	0.007
Na				0.023	0.023	0.015	0.014	0.002	
K				0.004	0.009		0.003		0.003
Zn	0.003	0.003	0.008	0.002	0.004	0.004	0.002	0.004	0.002
Cr					0.013	0.003		0.001	
Oxygens	24.000	24.000	24.000	24.000	24.000	24.000	24.000	24.000	24.000

Orthopyroxene

Sample	5303	5303	5243-2	5306	5306	5243-1	5243-1	5243-1
Location	D-2/3	D-3/1	E-1/3	G-1/1	G-1/2	H-1/2	H-1/5	H-1/6
SiO_2 (wt %)	50.19	50.15	49.97	52.56	52.73	53.29	53.56	52.06
TiO_2	0.08	0.13	0.13	0.08		0.12	0.02	0.45
Al_2O_3	7.77	8.00	8.37	1.65	1.50	1.19	1.57	1.85
FeO	15.7	16.32	17.96	26.25	24.84	16.62	16.14	5.46
MnO	0.13	0.22	0.10	0.74	0.73	0.30	0.27	0.12
MgO	24.21	23.94	22.75	18.78	19.81	26.73	26.93	14.47
CaO	0.10	0.06	0.13	0.54	0.47	0.40	0.36	23.78
Na_2O		0.07	0.11		0.02	0.01	0.03	0.46
K_2O	0.03	0.02			0.01			
ZnO			0.08			0.25	0.33	0.59
Cr_2O_3			0.25					
Total	98.21	98.91	98.86	100.61	100.11	98.92	99.22	99.24
Atoms								
Si	7.359	7.325	7.288	7.918	7.931	7.817	7.810	7.764
Ti	0.009	0.014	0.014	0.009		0.014	0.002	0.050
Al	1.343	1.378	1.439	0.293	0.266	0.206	0.270	0.326
Fe	1.926	1.994	2.190	3.308	3.125	2.039	1.968	0.680
Mn	0.016	0.028	0.013	0.094	0.094	0.038	0.033	0.015
Mg	5.290	5.212	4.946	4.217	4.441	5.845	5.853	3.216
Ca	0.016	0.010	0.020	0.088	0.076	0.063	0.057	3.799
Na		0.019	0.032		0.005	0.004	0.009	0.133
K	0.005	0.003			0.003		0.001	
Zn			0.008					
Cr			0.029			0.029	0.038	0.070
Oxygens	24.000	24.000	24.000	24.000	24.000	24.000	24.000	24.000

Phlogopite

Sample	**5301-1**	**5301-1**	**5301-2**	**5301-2**	**5301-1**	**5300-4**	**5300-4**	**5303**
Location	**A-2/2**	**A-3/3**	**B-1/3**	**B-2/1**	**B-4/3**	**C-1/3**	**C-2/3**	**D-2/4**
SiO_2 (wt %)	36.52	36.74	37.96	36.27	37.32	39.07	39.13	38.45
TiO_2	3.66	3.46	3.48	3.52	4.19	0.92	0.78	2.87
Al_2O_3	16.11	16.03	15.80	16.36	15.98	18.27	17.68	16.83
FeO	7.14	8.57	4.96	5.66	5.79	4.90	3.68	5.94
MnO			0.02		0.01			
MgO	18.36	17.76	20.80	19.40	19.27	22.39	21.94	19.58
CaO			0.04	0.02	0.01			0.02
Na_2O	0.13	0.11	0.28	0.45	0.31	0.21	0.18	0.14
K_2O	10.01	10.51	10.47	9.49	10.07	10.74	10.68	9.72
ZnO				0.03	0.05	0.03		
Cr_2O_3								
BaO	1.05	0.74	0.45	2.31	0.64			0.32
(Fe_2O_3)	(7.93)	(9.52)						
Total	92.99	93.93	94.26	93.51	93.64	96.54	94.08	93.86
	(93.78)	(94.88)						
Atoms								
Si	5.951	5.966	6.016	5.887	5.979	5.996	6.119	6.087
Ti	0.449	0.423	0.415	0.430	0.505	0.106	0.092	0.341
Al	3.094	3.068	2.952	3.130	3.018	3.305	3.260	3.140
Fe	0.973	1.164	0.658	0.768	0.775	0.629	0.481	0.786
Mn			0.002		0.002			
Mg	4.459	4.301	4.914	4.694	4.602	5.123	5.113	4.621
Ca			0.007	0.004	0.002			0.003
Na	0.041	0.036	0.086	0.142	0.097	0.063	0.055	0.044
K	2.081	2.178	2.117	1.965	2.058	2.104	2.130	1.962
Zn				0.004	0.006	0.003		
Cr								
Ba	0.067	0.047	0.028	0.147	0.040			0.020
Oxygens	24.000	24.000	24.000	24.000	24.000	24.000	24.000	24.000

Phlogopite

Sample	**5303**	**5243-2**	**5243-4**	**5243-4**	**5243-1**	**?**	**?**
Location	**D-4/3**	**E-1/1**	**F-1/3**	**F-2/1**	**H-1/1**	**I-1/3**	**I-2/2**
SiO_2 (wt %)	38.84	37.99	38.17	38.02	38.76	38.65	38.03
TiO_2	2.28	3.92	4.82	4.68	4.98	3.00	2.47
Al_2O_3	17.16	15.75	15.59	15.60	13.00	17.09	16.65
FeO	6.81	8.25	9.99	6.90	6.70	7.18	8.24
MnO	0.02	0.02	0.02		0.01	0.05	0.06
MgO	19.54	17.94	18.58	20.01	20.06	20.28	19.70
CaO	0.02				0.05		
Na_2O	0.15	0.03	0.17	0.15	0.16	0.29	0.26
K_2O	8.76	10.43	10.13	10.07	9.84	9.93	9.83
ZnO		0.04					
Cr_2O_3		0.37	0.04	0.01	0.79	0.01	0.01
BaO	0.11	0.14	0.11	0.09	0.04	0.18	0.18
(Fe_2O_3)							
Total	93.69	95.08	97.6	95.54	94.39	96.66	95.42
Atoms							
Si	6.124	6.047	5.952	5.969	6.162	5.985	6.000
Ti	0.270	0.470	0.565	0.553	0.595	0.349	0.293
Al	3.192	2.954	2.864	2.887	2.436	3.120	3.096
Fe	0.898	1.098	1.302	0.906	0.891	0.930	1.087
Mn	0.003	0.002	0.003		0.001	0.007	0.008
Mg	4.596	4.255	4.318	4.682	4.755	4.680	4.633
Ca	0.004	0.001			0.008		
Na	0.046	0.076	0.052	0.045	0.050	0.087	0.080
K	1.764	2.118	2.015	2.016	1.996	1.962	1.978
Zn		0.004					
Cr		0.046	0.004	0.001	0.099	0.001	0.001
Ba	0.007	0.009	0.006	0.005	0.003	0.011	0.011
Oxygens	24.000	24.000	24.000	24.000	24.000	24.000	24.000

Cordierite

Sample	**5301-1**	**5301-1**	**5301-1**	**5303**	**5303**	**5303**	**?**
Location	**A-1/2**	**A-2/3**	**A-3/2**	**D-3/4**	**D-3/2**	**D-4/4**	**I-1/1**
SiO_2 (wt %)	49.16	49.11	49.27	49.46	49.24	49.27	48.82
TiO_2							0.01
Al_2O_3	33.54	33.40	33.68	33.53	33.55	33.37	33.47
FeO	2.21	2.09	2.50	2.71	2.68	2.46	2.45
MnO	0.05	0.04	0.03	0.03	0.04	0.01	0.04
MgO	12.11	12.18	11.98	11.76	11.78	11.87	11.98
CaO	0.03	0.01		0.02	0.01	0.06	
Na_2O	0.13	0.13	0.07	0.03	0.03	0.04	0.06
K_2O		0.04	0.01	0.02	0.02	0.02	
ZnO							
Cr_2O_3	0.06		0.07				0.01
Total	97.28	96.99	97.62	97.53	97.34	97.1	96.85
Atoms							
Si	6.637	6.645	6.635	6.666	6.652	6.665	6.625
Ti							0.001
Al	5.336	5.327	5.346	5.326	5.342	5.321	5.354
Fe	0.250	0.236	0.282	0.305	0.302	0.279	0.278
Mn	0.006	0.005	0.004	0.004	0.004	0.001	0.005
Mg	2.436	2.457	2.404	2.362	2.371	2.394	2.424
Ca	0.004	0.001		0.002	0.002	0.008	
Na	0.033	0.034	0.019	0.009	0.007	0.011	0.016
K		0.007	0.003	0.003	0.004	0.004	
Zn							
Cr	0.006		0.007				0.001
Oxygens	24.000	24.000	24.000	24.000	24.000	24.000	24.000

Garnet

Sample	**5303**	**5303**	**5243-7**
Location	**D-1/2**	**D-2/5**	**F-2/2**
SiO_2 (wt %)	40.94	39.98	40.05
TiO_2	0.01	0.05	0.02
Al_2O_3	22.99	22.63	22.65
FeO	20.73	22.45	23.04
MnO	0.80	0.81	1.10
MgO	14.53	13.41	12.92
CaO	1.00	0.93	0.66
Na_2O			0.04
K_2O			
ZnO			
Cr_2O_3			
Total	101.00	100.25	100.47
Atoms			
Si	6.017	5.978	5.994
Ti	0.001	0.006	0.002
Al	3.984	3.988	3.995
Fe	2.548	2.808	2.884
Mn	0.099	0.103	0.139
Mg	3.183	2.989	2.882
Ca	0.158	1.149	0.105
Na			0.010
K			
Zn			
Cr			
Oxygens	24.000	24.000	24.000

Plagioclase

Sample	**5301-1**	**5303**	**5303**	**5303**	**5306**	**5243-1**
Location	**A-1/3**	**D-1/1**	**D-3/5**	**D-4/5**	**G-1/5**	**H-1/3**
SiO_2 (wt %)	56.31	62.22	61.87	61.71	52.47	45.67
TiO_2					0.10	
Al_2O_3	27.88	24.72	24.95	24.79	30.62	35.08
FeO	0.15	0.08	0.03	0.12	0.28	0.23
MnO						0.02
MgO						0.05
CaO	9.29	5.70	5.71	5.57	13.31	17.80
Na_2O	6.22	8.27	8.30	8.25	3.72	1.29
K_2O	0.31	0.46	0.33	0.36	0.16	0.24
ZnO						
Cr_2O_3						
BaO						
P_2O_5						
Total	100.15	101.46	101.19	100.81	100.67	100.37
Atoms						
Si	7.583	8.176	8.147	8.158	7.097	6.295
Ti					0.010	
Al	4.425	3.829	3.873	3.863	4.881	5.699
Fe	0.017	0.009	0.003	0.014	0.032	0.026
Mn						0.002
Mg					0.001	0.011
Ca	1.341	0.802	0.806	0.789	1.929	2.628
Na	1.624	2.108	2.119	2.114	0.974	0.345
K	0.053	0.078	0.056	0.061	0.028	0.042
Zn						
Cr						
Ba						
Oxygens	24.000	24.000	24.000	24.000	24.000	24.000

	Potash feldspar			Sillimanite	
Sample	**5300-4**	**5303**	**5303**	**5303**	**5303**
Location	**C-1/2**	**D-3/6**	**D-4/6**	**D-2/2**	**D-4/2**
SiO_2 (wt %)	63.69	64.22	64.14	36.65	36.67
TiO_2	0.02			0.03	0.03
Al_2O_3	19.18	18.31	18.32	62.11	62.00
FeO	0.09			0.97	0.55
MnO					
MgO	0.12			0.21	0.19
CaO	0.10	0.11	0.17	0.04	0.02
Na_2O	1.85	1.81	2.00		
K_2O	13.93	13.58	13.31	0.01	0.02
ZnO	0.01				
BaO		1.45	1.31		
SrO		0.04	0.04		
Total	98.99	99.52	99.29	100.01	99.49
Atoms					
Si	8.868	8.964	8.959	4.772	4.788
Ti	0.002			0.003	0.003
Al	3.147	3.012	3.017	9.532	9.543
Fe	0.011			0.105	0.060
Mn					
Mg	0.125			0.040	0.038
Ca	0.015	0.016	0.026	0.006	0.002
Na	0.498	0.490	0.542		
K	2.474	2.419	2.371	0.001	0.004
Zn	0.001				
Ba		0.080	0.071		
Sr		0.003	0.003		
Oxygens	24.000	24.000	24.000	24.000	24.000

	Rutile		Hornblende	Apatite	Ilmenite
Sample	**5301-1**	**5301-2**	**5243-1**	**5301-2**	**5306**
Location	**A-1/5**	**B-2/4**	**H-1/4**	**B-1/6**	**G-1/3**
SiO_2 (wt %)			44.05	0.30	
TiO_2	99.26	100.02	2.24		51.77
Al_2O_3			11.08		0.29
FeO	0.48	0.66	7.73	0.15	46.02
MnO	0.01	0.03	0.04	0.06	0.58
MgO			14.41	0.18	0.52
CaO	0.04	0.01	12.66	53.86	
Na_2O			1.20		
K_2O			2.29		
CuO					Cr 0.03
BaO					V 0.47
P_2O_5			Cr 1.18	41.16	
Cr_2O_3					
Total	99.8	100.71	96.88	95.7	99.69
Atoms					
Si			6.750	0.049	
Ti	11.963	11.954	0.258		7.854
Al			2.000		0.069
Fe	0.065	0.088	0.991	0.021	7.765
Mn	0.001	0.004	0.005	0.008	0.099
Mg			3.292	0.044	0.158
Ca	0.008	0.001	2.079	9.495	
Na			0.358		
K			0.448		
Zn					Cr 0.005
Ba					V 0.299
Cr			Cr 0.143	5.733	
Oxygen	24.000	24.000	24.000	24.000	24.000

	Magnetite	Vermiculite	Pyrite	Chalcopyrite
Sample	**5306**	**5301-1**	**?**	**5243-4**
Location	**G-1/4**	**B-4/1**	**I-2/3**	**F-1/4**
SiO_2 (wt %)		36.19	S 53.49	S 35.12
TiO_2	0.19			ZnO 0.01
Al_2O_3	0.42	18.23		
FeO	90.36	19.63	46.51	30.61
MnO		0.37		
MgO		11.19		
CaO		1.90		
Na_2O				
K_2O		0.28		
CuO	Cr 0.71	0.03		34.25
BaO	V 1.50			
P_2O_5				
Cr_2O_3				
Total	93.18	87.83	100.00	100.00
Atoms				
Si		6.193		
Ti	0.043			
Al	0.147	3.676		Cu 0.539
Fe	22.696	2.809	0.832	0.548
Mn		0.054	S 1.666	S 1.094
Mg		2.853		
Ca		0.349		
Na				
K		0.061		
Zn	Cr 0.167	0.004		
Ba	V 0.299			
Cr				
Oxygen	24.000	24.000	0.000	0.000